AC/DC pulsed power corona

Smits, G.J.

Award date:
2006

TU/e technische universiteit eindhoven

Capaciteitsgroep Elektrische Energietechniek
Electrical Power Systems

AC/DC Pulsed Power Corona

door: G.J. Smits
EPS.06.A.185

Afstudeerwerk verricht o.l.v.:

prof.dr.ir. J.H. Blom
dr.ing. A.J.M. Pemen

december 2006

Abstract

A new generation of process technology of cleaning gas, air and water is represented by pulsed corona these days. It's based on electric process technology by using modulated high-voltage power with electronic gas discharge (corona) as an interface. The current pulsed corona circuits consist of quit a lot of high-voltage components and these components are expensive. This resulted in new ideas for pulsed corona circuits with less high-voltage components. The new circuit needed to be tested as well as a new patent circuit for magnetic pulse compression [1]. This master thesis shows the results of the different experiments, conclusions and recommendations for further work.

The experiments were done with an AC/DC/Pulse source which consists of a two-stage resonant charging circuit switched by thyristors, a transformer, and the corona reactor. Voltage pulses of 30 to 35 kV with a rise time of about $10\mu s$, a pulse duration of 3 ms, a pulse repetition rate of 500 pulses per second (pps), and an energy of up to 1.1 J/pulse have been achieved. The experiments were done with different types of corona reactor, the one compartment corona reactor, the two compartment corona reactor and the two compartment magnetic pulsed compressed corona reactor. The plate distances of the compartments were changed between 9, 10 and 11 cm. The magnetic pulsed compressed corona reactor is based on a patent [1] in which the compartments of the corona reactor are used for the pulse compression. The ozone productions are measured and also the ozone yield per corona reactor is determined.

The results show that the performance of the one compartment corona reactor and the two compartment corona are about the same. The two compartment magnetic pulsed compressed corona reactor has a better efficiency compared to the two compartment corona reactor and a shorter rise time of the pulse voltage. The amount of energy is higher but the ozone yield of the two compartment magnetic pulsed compressed corona reactor is lower.

Contents

1 Introduction **4**

1.1 Objectives 5

1.2 Outline 6

2 The circuit **7**

3 Model **10**

3.1 Introduction 10

3.2 First step 10

3.2.1 Current calculations 10

3.2.2 Voltage calculations 12

3.3 Second Stage 15

3.3.1 Current calculations 15

3.3.2 Voltage calculations 16

3.4 Discharging Corona 19

3.5 Magnetic pulse compression 19

3.6 Matching 23

4 Experimental test results **26**

4.1 Typical waveforms 26

4.2 One compartment corona reactor 32

4.2.1 Plate distance 9 cm 32

4.2.2 Plate distance 10 cm 34

4.2.3 Plate distance 11 cm 35
4.3 Two compartment corona reactor 36
4.4 Efficiency 40
4.5 Two compartment mpc corona reactor 41
4.5.1 Energy 41
4.5.2 Currents and Voltages 43
4.5.3 Ozone 50

5 Conclusions and Recommendations **53**
5.0.4 Conclusions 53
5.0.5 Recommendations 54

Bibliography **55**

A Table of component values **58**

B Matlab formulas **60**

Chapter 1

Introduction

A new generation of process technology of cleaning gas, air and water is represented by pulsed corona these days. It's based on electric process technology by using modulated high-voltage power with electronic gas discharge (corona) as an interface. This corona produces among other things electrons, ions, radicals and ultraviolet radiation which can be used for the cleaning process. The active parts make it possible that among other things hydrocarbons and odor will be converted, micro-organisms will be inactivated and fine-grain dust will be filtered out of the air. This technology can be used for air cleaning (reduction of odor, fine-grain dust and volatile chemical components), cleaning of combustion gases (fine-grain dust, NOx, SOx, heavy metals and dioxides), inactivation of micro-organisms and viruses in air and water and sewage cleaning (phenol, organic components). In the future the process can also be used for plasma activated catalysts, biogas conditioning, plasma conversion and plasma combustion.

An advantage of this process technology is that it can be used in any kind of branch industry where cleaning of gas, air or water is desirable. In comparison with other cleaning processes the main advantages of cleaning by pulsed corona are:

- It's fully electronic: energy can be saved because the high efficiency makes sure that almost all the electric energy is converted into chemical (cleaning) energy.
- Multiple use: a combination of cleaning, conversion and inactivation of harmful components can be done at the same time.
- Insensitive for process conditions and the process itself. It's easy to combine it with other technologies as well, on small or large scale processes it doesn't matter it can be customized to the process.
- There is no emission of harmful rest products.
- No harmful chemicals are necessary.

- An easy to control mechanism.

But besides the advantages there are also some disadvantages with a pulsed corona system. The high power, modulating high voltage source needs to match with the corona reactor to get the best efficiency. There is already done some successful research with sources that can reach up to 17 kW and an energy efficiency of 90% but there are still some cons. The biggest cons are the high investment cost (in the order of 20-30kEuro per kW corona power) and short lifespan of the high voltage switches, to be more specific:

- High voltage switches are based on the principle of the multi coaxial gas-triode sparkgap [2]. These switches are known for: suitable impedance, short rise time, high capability, repetitive. There are good results reached but there are still some disadvantages. At a high repetitive frequency (>300 pps) there needs to be a high flow of dry air. Due to this the practical part will be harder to achieve and more expensive. Also the electrodes need to be replaced after a use of 4 years of continuous process.
- Expensive high voltage capacitors: in the existing pulse sources all the energy has to be stored in high voltage capacitors during each pulse and will be discharged by a high voltage switch and a pulse shaping network to the corona reactor.

A solution for this problem is an AC/DC/Pulse modulation. This concept is different compared to the regular pulse source because there are no expensive, complex electric components needed (like high voltage switches, high voltage capacitors and pulse shaping networks) and the amount of high voltage components is minimized. Unless all these changes the outcome is the same as with the conventional concept, but the investment costs of this pulsed corona system are distinguish lower. In the concept two different topologies will be combined, namely the high voltage resonator to create the AC/DC voltage and a magnetic pulse compressor to create the pulsed high voltage. This combination of circuits consists of a minimum amount of high voltage components which is a big plus for this system. In the AC/DC/Pulse modulation concept the two high voltage capacitors are substituted by the corona reactor itself. The reactor can be modeled as an capacitance and so it can replace the high voltage capacitors. The reactor will be divided into two sections which will be connected by the same saturable inductor as used with the conventional magnetic pulse compressor, this new network forms a simple but efficient pulse compressor.[3],[4]

1.1 Objectives

The main objective of this master project is to realize with experiments an optimized process with a high efficient energy conversion to ozone production. Due to the experiments and a model the ideal values for the different capacitors and inductors can be realized. Another objective is to realize an amount

of compression by using magnetic pulse compression two corona reactor compartments. If another way of pulse compression would be used the main advantage of the AC/DC/Pulse system, less high-voltage components, would go lost. For example if a TLT system would be used this would mean that there is also an extra DC-source needed and extra high-voltage components.

1.2 Outline

This report will be an overview of the first experiments done with AC/DC/Pulse modulation. In the second chapter the circuit will be explained by taking the circuit. The analytical model will be discussed in chapter 3, were the AC/DC source, the magnetic pulse compression and matching will be made clear. In the fourth chapter the results of the experiment with the AC/DC source and the corona reactor will be given to show what the influence is of different capacitance (C_L) and the plate distance of the compartment of the corona reactor. Also the magnetic pulse compression results will be shown and discussed. In the last chapter the results will be taken together to make a final conclusion and recommendations for future work will be made.

Chapter 2

The circuit

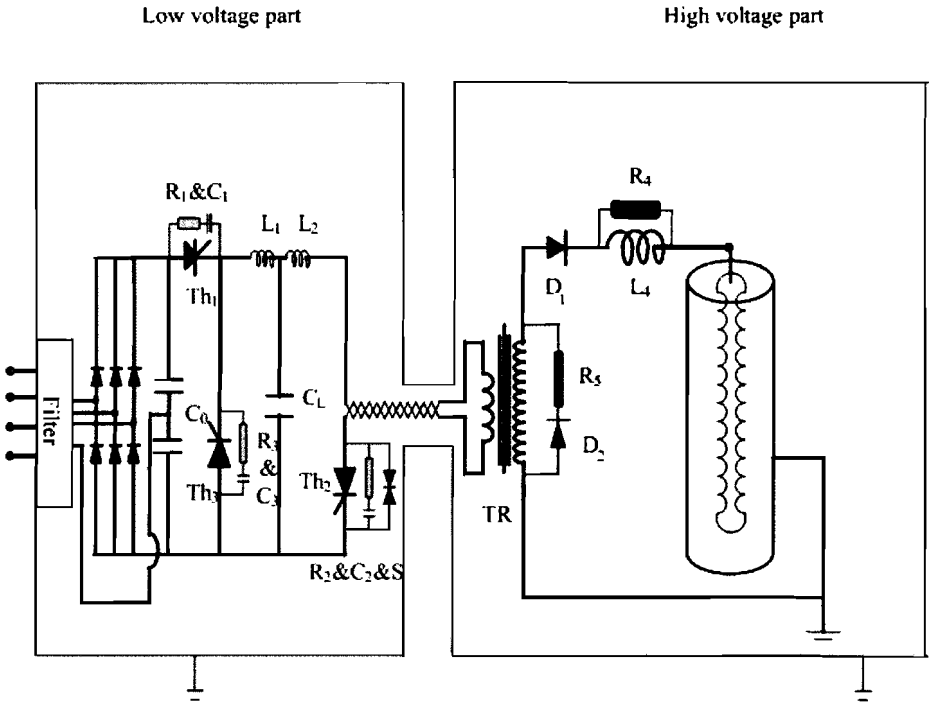

Figure 2.1: The AC/DC/Pulse circuit

Figure 2.1 shows a schematic diagram of the main electrical circuit with the corona reactor. The pulse transformer TR separates the low and high voltage parts of the circuit. The low-voltage part mainly consists of a main filter, a set of rectifiers, three air-core inductors L_1, L_2, three thyristors Th_1, Th_2, and Th_3, two energy storage capacitors C_0 (which consists out of two capacitors connected in series) and C_L, and primary windings of the pulse transformer TR. The three thyristors are switched consecutively in order to charge the corona

reactor. As indicated in Fig.2.1, three RC snubbers and one silicon-surge voltage suppressor S are used for avoiding overvoltage on these thyristors.

The high-voltage part mainly consists of secondary windings of the pulse transformer TR, two high-voltage diodes D_1 and D_2, two damping resistors R_4 and R_5, an air-core inductor L_4. The free wheeling diode D_2 together with the damping resistor R_5 is designed to protect the high-voltage diode D_1. A RC snubber is used to protect the diode D_1 during normal operation. Electronic control systems for triggering the thyristors and electrical diagnostic system for voltage and current measurements are the same as in a previous design (Smulders et al. 1998, van Heesch and van der Laan 2000).

A two-step process generates the high-voltage pulse. In the first step, the low-voltage capacitor C_L is resonantly charged via the energy storage capacitor C_0, the thyristor Th_1, and the inductor L_1, where $C_0 \gg C_L$. During the second step, the high-voltage corona reactor is resonantly charged via C_L, L_2, TR, Th_2, D_1, and L_4. Before the low-voltage capacitor C_L is recharged again, the third thyristor Th_3 is used to correct the voltage polarity on C_L via Th_3 and L_1.

After the high-voltage corona reactor is charged via C_L, L_2, TR, Th_2, $D1$ and $L4$, the discharging takes place inside the reactor itself, which forms a RC-network and discharges to V_{dc}.

Figure 2.2 shows a schematic diagram of a time-resolved voltage waveform on the capacitor C_L, where arrows of Th_1, Th_2, and Th_3 refer to the moments at which the corresponding thyristor is closed. The voltages V_n and $V_{(n+1)}$ refer to the n^{th} and $(n+1)^{th}$ voltage levels on C_L after the first step resonant charging. The voltage ΔVn refers to the voltage on C_L after the second step resonant charging. The n is the pulse sequence number.[5],[6]

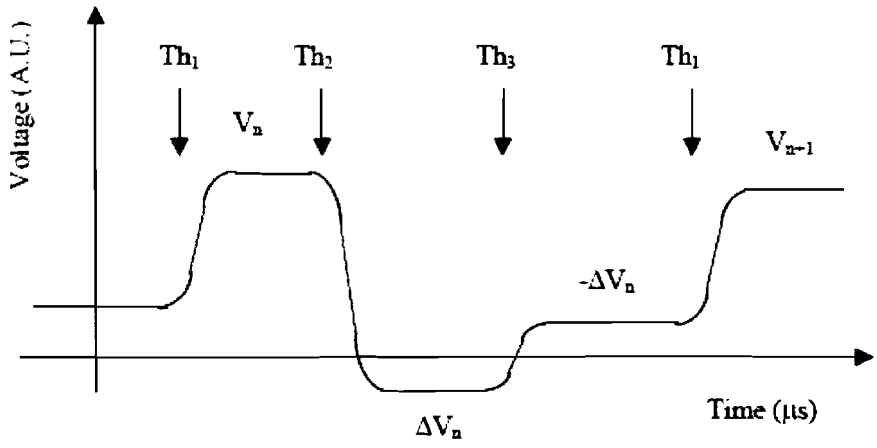

Figure 2.2: A schematic diagram of a time-resolved voltage waveform on the capacitor C_L. The arrows refer to the moments at which the corresponding thyristor is closed.

Table 2.1: Main specifications of the fast switching-off ABB thyristor.

Main Specification	Main Specifications	
V_{DRM}, V_{RRM}	2000 V	
Voltage rate $\frac{dV}{dt_{crit}}$ at turn-off	$1000V/\mu s$	
Current rate $\frac{di}{dt_{crit}}$ at turn-on	$300A/\mu s$	continuous
Max average on-state current I_{TAVM}	1270 A	
Max RMS on-state current I_{TRMS}	2000 A	
Limiting load integral I^2t	$1125kA^2s$	at 10 ms
Threshold voltage V_{TO}	1.25 V	
On-state voltage V_T	2.1 V	at 2000 A
Slope resistance R_T	$0.42m\omega$	600-1800 A
Holding current I_H	30 70 mA	at 25^oC
Latching current I_L	150-600 mA	
Turn off time t_1	$\leq 60\mu s$	
Delay time t_d	$\leq 2\mu s$	$V_d = 0.4V_{DRM}$
Recovery charge Q	$-560\mu C$	

In chapter 4 the typical output waveforms of the AC/DC/Pulse source and the corona reactor will be shown and discussed.

In order to make sure that the thyristors are able to switch at the given moment shown in figure 2.2, they have to meet with some qualities. Requirements like fast switching-off in order to achieve high repetition rates. Moreover, the maximum on-state average current and the maximum on-state mean square root current should be chosen as about 2 times larger than the operating values. Table 2.1 lists one example of the main specifications of the thyristor used for the present work.[5]

Chapter 3

Model

3.1 Introduction

In this chapter the circuit in figure 2.1 will be analytical described. The first step (chapter 3.2) will deal with the resonant charging of the low-voltage capacitor C_L via the energy storage capacitor C_0, the thyristor Th_1, and the inductor L_1, where $C_0 \gg C_L$. Chapter 3.3 will describe the second step of the AC/DC/Pulse source. The resonantly charging of the high-voltage corona reactor via C_L, L_2, TR, Th_2, D_1, and L_4. The model of the discharging of the corona will be discussed in chapter 3.4. In appendix A table A.1 the components values used for the analytical model are given.

3.2 First step

3.2.1 Current calculations

For the circuit of the AC/DC/Pulse power source the basics come from the general solution for the natural undamped current. I_1 is the current in circuit $C_0 - Th_1 - L_1 - C_L$.

$$I_1(t_1) = A_{I1} \cdot e^{-\alpha_1 \cdot t_1} \cdot \sin(\omega_1 \cdot t_1 + \phi_1) \tag{3.1}$$

For calculation of the different values of the analytical model, some measured values are used.

For the circuit applies: $I_1(0) = 0$

From the equation: $I_1(0) = A_{I1} \cdot \sin(\phi_1)$

This results in:

$$A_{I1} \cdot sin\phi_1 = 0 \quad \text{therefore:} \quad \phi_1 \equiv 0$$

The series impedance function for current analysis is:

$$Z(s) = \frac{1}{s \cdot C_0} + s \cdot L_1 + \frac{1}{s \cdot C_L} \tag{3.2}$$

$$Z(s) = \frac{s^2 \cdot L_1 \cdot C_0 \cdot C_L + C_0 + C_L}{s \cdot C_0 \cdot C_L} \tag{3.3}$$

$$C_{T1} = \frac{1}{\frac{1}{C_0} + \frac{1}{C_L}} \tag{3.4}$$

For calculation of the impedance zero's for the natural undamped current the next equations are used:

$$\alpha_1 = \frac{R}{2 \cdot L_1} \tag{3.5}$$

$$\omega_{01} = \frac{1}{\sqrt{L_1 \cdot C_{T1}}} \tag{3.6}$$

$$\omega_1 = \sqrt{\omega_{01}^2 - \alpha_1^2} \tag{3.7}$$

$$s_1 = -\alpha_1 + \omega_1 \qquad s_2 = -\alpha_1 - \omega_1 \tag{3.8}$$

$$\phi_1 = \arctan \frac{\alpha_1}{\omega_1} \tag{3.9}$$

Differentiation of equation 3.1 gives:

$$\begin{aligned} \tfrac{d}{dt_1} A_{I1} \cdot e^{\alpha_1 \cdot t_1} \cdot \sin(\omega_1 \cdot t_1 + \phi_1) \quad = \\ -A_{I1} \cdot \alpha_1 \cdot e^{-\alpha_1 \cdot t_1} \cdot \sin(\omega_1 \cdot t_1 + \phi_1) \\ +A_{I1} \cdot e^{-\alpha_1 \cdot t_1} \cdot \cos(\omega_1 \cdot t_1 + \phi_1) \cdot \omega_1 \end{aligned} \tag{3.10}$$

Determine the initial derivative of the current in the circuit at $t_1 = 0$ with $\phi_1 = 0$ gives:

$$\frac{d}{dt_1} I_1(0) = -A_{I1} \cdot \alpha_1 \cdot e^{-\alpha_1 \cdot 0} \cdot \sin(\omega_1 \cdot 0 + 0) + A_{I1} \cdot e^{-\alpha_1 \cdot 0} \cdot \cos(\omega_1 \cdot 0 + 0) \cdot \omega_1$$

$$\frac{d}{dt_1} I_1(0) = A_{I1} \cdot \omega_1 \tag{3.11}$$

Keeping in mind that C_0 is initially charged to $V_{dc} \Rightarrow V_{C_0}(0) = V_{dc}$:

$$\frac{d}{dt_1} I_1(0) = \frac{V_{C_0}(0)}{L_1} \tag{3.12}$$

Equating again yields:

$$A_{I1} = \frac{V_{C_0}(0)}{\omega_1 \cdot L_1} \tag{3.13}$$

With:

$$\omega_1 = \frac{1}{\sqrt{L_1 \cdot C_{T1}}}$$

Substituting ω_1 in equation 3.13 yields:

$$A_{I1} = \frac{V_{C_0}(0) \cdot \sqrt{L_1 \cdot C_{T1}}}{L_1} \qquad \Rightarrow \qquad A_{I1} = V_{C_0}(0) \cdot \sqrt{\frac{C_{T1}}{L_1}} \tag{3.14}$$

Filling in all the variables in formule 3.1 gives the solution for the natural undamped current:

$$I_1(t_1) = V_{C_0}(0) \cdot \sqrt{\frac{C_{T1}}{L_1}} \cdot e^{-\alpha_1 \cdot t_1} \cdot \sin(\omega_1 \cdot t_1) \tag{3.15}$$

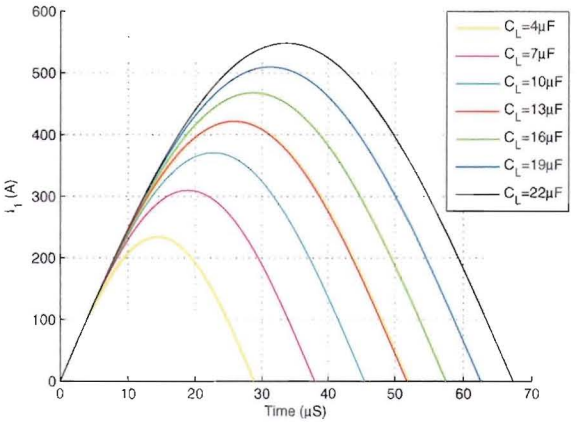

Figure 3.1: Plot of first stage of I_1 model with $C_0 \gg C_L$

3.2.2 Voltage calculations

For the calculations of the voltages on the capacitors the equations can be converted by integrating the current-equation (3.15).

$$V_{C_0}(t_1) = \frac{1}{C_0} \cdot \int_0^{t_1} I_1(\tau_1) d\tau_1 \tag{3.16}$$

$$V_{C_0}(t_1) = \frac{1}{C_0} \cdot \int_0^{t_1} A_{I1} \cdot e^{-\alpha_1 \cdot \tau_1} \cdot \sin(\omega_1 \cdot \tau_1) d\tau_1 \tag{3.17}$$

$$V_{C_0}(t_1) = \frac{A_{I1}}{C_0} \cdot \int_0^{t_1} e^{-\alpha_1 \cdot \tau_1} \cdot \sin(\omega_1 \cdot \tau_1) d\tau_1 \tag{3.18}$$

Consider the integral alone:

$$\begin{aligned} & \int_0^{t_1} e^{-\alpha_1 \cdot \tau_1} \cdot \sin(\omega_1 \cdot \tau_1) d\tau_1 \\ = & \frac{-\omega_1 \cdot e^{-\alpha_1 \cdot t_1} \cdot \cos(\omega_1 \cdot t_1) + \alpha_1 \cdot e^{-\alpha_1 \cdot t_1} \cdot \sin(\omega_1 \cdot t_1) - \omega_1}{(\alpha_1^2 + \omega_1^2)} \\ = & \frac{-(e^{-\alpha_1 \cdot t_1} \cdot \omega_1 \cdot \cos(\omega_1 \cdot t_1) + e^{-\alpha_1 \cdot t_1} \cdot \alpha_1 \cdot \sin(\omega_1 \cdot t_1) - \omega_1)}{(\alpha_1^2 + \omega_1^2)} \end{aligned} \tag{3.19}$$

We have: $\omega_1^2 = \omega_{10}^2 - \alpha_1^2$

From Pythagoras' Theorem: $\phi_1 = \arctan(\frac{\alpha_1}{\omega_1})$
Therefore:

$$\begin{aligned} \omega_1 &= \omega_{10} \cdot \cos(\phi_1) \\ \alpha_1 &= \omega_{10} \cdot \sin(\phi_1) \\ \omega_{10} &= \sqrt{\omega_1^2 + \alpha_1^2} \end{aligned}$$

Reducing equation 3.19 to:

$$\frac{-(e^{-\alpha_1 \cdot t_1} \cdot \omega_{10} \cdot \cos(\phi_1) \cdot \cos(\omega_1 \cdot t_1) + e^{-\alpha_1 \cdot t_1} \cdot \omega_{10} \cdot \sin(\phi_1) \cdot \sin(\omega_1 \cdot t_1) - \omega_1)}{\omega_{10}^2}$$
$$or$$
$$\frac{-[e^{-\alpha_1 \cdot t_1} \cdot \omega_{10} (\cdot \cos(\phi_1) \cdot \cos(\omega_1 \cdot t_1) + \sin(\phi_1) \cdot \sin(\omega_1 \cdot t_1)) - \omega_1]}{\omega_{10}^2}$$
$$or$$
$$-\frac{e^{-\alpha_1 \cdot t_1} \cdot \omega_{10} \cdot \cos(\omega_1 \cdot t_1 - \phi_1) - \omega_1}{\omega 10^2} \tag{3.20}$$

Because $\alpha_1 = 0Hz$ gives that $\omega_{10} = \omega_1$ this will result in that equation 3.21 can be written as follows:

$$-\frac{\omega_1 \cdot \cos(\omega_1 \cdot t_1) - \omega_1}{\omega_1^2} \tag{3.21}$$

V_{C_0} is already precharged to $V_{C_0}(= V_{dc})$ and can only discharge during state 1. The complete equation for the voltages on the capacitors can be written as a combination of the initial value V_{C_0} with equation 3.21 subtracted:

$$V_{C_0}(t_1) = V_{C_0}(0) + \frac{A_{I1}}{C_0} \cdot \frac{\omega_1 \cdot \cos(\omega_1 \cdot t_1) - \omega_1}{\omega_1^2} \tag{3.22}$$

Due to the fact that the same current is going through C_L. V_{C_L} can be derived from equation 3.22.

$$V_{C_L}(t_1) = -\frac{A_{I1}}{C_L} \cdot \frac{\omega_1 \cdot \cos(\omega_1 \cdot t_1) - \omega_1}{\omega_1^2} \tag{3.23}$$

The first stage will start when thyristor 1 (Th_1) starts to conduct after V_{C_0} has reached it's maximum. The first stage will stop when the voltage on Th_1 applies with $VTh_1 \leq 0$. The voltage on V_{C_L} will remain till the second stage starts. The voltage on V_{C_0} will hardly change due to the fact that $C_L \ll C_0$, and besides that C_0 get constantly charged for the net.

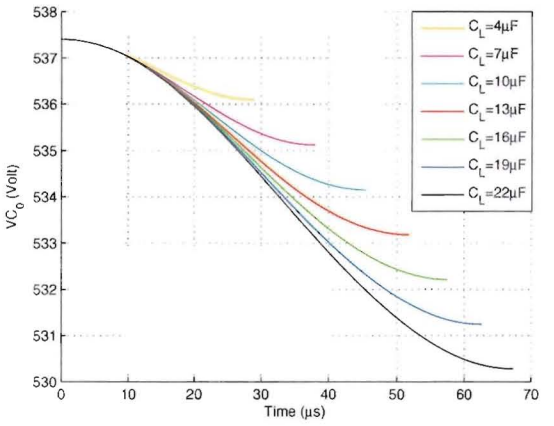

Figure 3.2: Plot of first stage of V_{C_0} model with $C_0 \gg C_L$

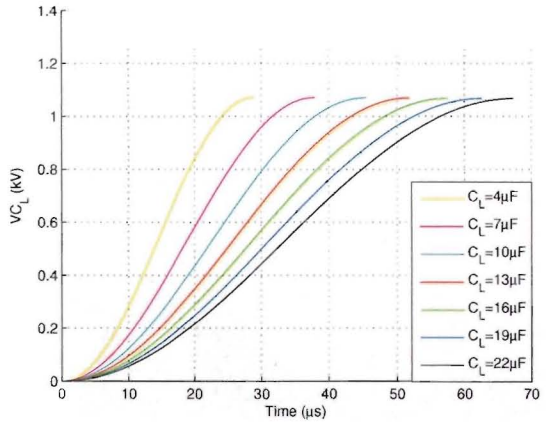

Figure 3.3: Plot of first stage of V_{C_L} model with $C_0 \gg C_L$

3.3 Second Stage

3.3.1 Current calculations

The second stage is the part were C_L discharges to the corona reactor. The current shape of I_2, which is the current C_L, L_2, TR, Th_2, D_1, L_4 and R_4, is the same as that from the first stage so equation 3.24 is the same as equation 3.1:

$$I_2(t_2) = A_{I2} \cdot e^{-\alpha_2 \cdot t_2} \cdot \sin(\omega_2 \cdot t_2 + \phi_2) \tag{3.24}$$

The initial value is also the same as with the first stage:

For the circuit applies: $I_2(0) = 0$

From the equation: $I_2(0) = A_{I2} \cdot \sin(\phi_2)$

This results in:

$$A_{I2} \cdot sin\phi_2 = 0 \quad \text{therefore:} \quad \phi_2 \equiv 0$$

The series impedance function for current analysis is:

$$Z(s) = \frac{1}{s \cdot C_L} + s \cdot L_2 + \frac{1}{s \cdot C_{Corona}} \tag{3.25}$$

$$Z(s) = \frac{s^2 \cdot L_2 \cdot C_L \cdot C_{Corona} + C_L + C_{Corona}}{s \cdot C_0 \cdot C_{Corona}} \tag{3.26}$$

$$C_{T2} = \frac{1}{\frac{1}{C_L} + \frac{1}{C_{Corona}}} \tag{3.27}$$

For calculation of the impedance zero's for the natural undamped current the next equations are used:

$$\alpha_2 = \frac{R}{2 \cdot L_2} \tag{3.28}$$

$$\omega_{02} = \frac{1}{\sqrt{L_2 \cdot C_{T2}}} \tag{3.29}$$

$$\omega_2 = \sqrt{\omega_{02}^2 - \alpha_2^2} \tag{3.30}$$

$$s_1 = -\alpha_2 + \omega_2 \qquad s_2 = -\alpha_2 - \omega_2 \tag{3.31}$$

$$\phi_2 = \arctan \frac{\alpha_2}{\omega_2} \tag{3.32}$$

Differentiation of equation 3.24 gives:

$$\begin{aligned} \tfrac{d}{dt_2} A_{I2} \cdot e^{\alpha_2 \cdot t_2} \cdot \sin(\omega_2 \cdot t_2 + \phi_2) \quad = \\ -A_{I2} \cdot \alpha_2 \cdot e^{-\alpha_2 \cdot t_2} \cdot \sin(\omega_2 \cdot t_2 + \phi_2) \\ +A_{I2} \cdot e^{-\alpha_2 \cdot t_2} \cdot \cos(\omega_2 \cdot t_2 + \phi_2) \cdot \omega_2 \end{aligned} \tag{3.33}$$

Determine the initial derivative of the current of the circuit at $t_2 = 0$ with $\phi_2 \approx 0$ gives:

$$\frac{d}{dt_2} I_2(0) = -A_{I2} \cdot \alpha_2 \cdot e^{-\alpha_2 \cdot 0} \cdot \sin(\omega_2 \cdot 0 + 0) + A_{I2} \cdot e^{-\alpha_2 \cdot 0} \cdot \cos(\omega_2 \cdot 0 + 0) \cdot \omega_2$$

$$\frac{d}{dt_2} I_2(0) = A_{I2} \cdot \omega_2 \tag{3.34}$$

Keeping in mind that C_L is initially charged to $V_{C_L}(0) \Rightarrow V_{C_L}(0) = 2 \cdot V_{dc}$ due to the fact that $C_L \ll C_0$:

$$\frac{d}{dt_2} I_2(0) = \frac{V_{C_L}(0)}{L_2} \tag{3.35}$$

Equating again yields: $$A_{I2} = \frac{V_{C_L}(0)}{\omega_2 \cdot L_2} \tag{3.36}$$

With: $$\omega_2 = \frac{1}{\sqrt{L_2 \cdot C_{T2}}}$$

Substituting ω_2 in equation 3.35 yields:

$$A_{I2} = \frac{V_{C_L}(0) \cdot \sqrt{L_2 \cdot C_{T2}}}{L_2} \quad \Rightarrow \quad A_{I2} = V_{C_L}(0) \cdot \sqrt{\frac{C_{T2}}{L_2}} \tag{3.37}$$

Filling in all the variables in equation 3.24 gives the solution for the natural undamped current:

$$I_2(t_2) = V_{C_L}(0) \cdot \sqrt{\frac{C_{T2}}{L_2}} \cdot e^{-\alpha_2 \cdot t_2} \cdot \sin(\omega_2 \cdot t_2) \tag{3.38}$$

3.3.2 Voltage calculations

For the calculations of the voltages on the capacitors the equations can be converted by integrating equation 3.39.

$$V_{C_L}(t_2) = \frac{1}{C_L} \cdot \int_0^{t_2} I_2(\tau_2) d\tau_2 \tag{3.39}$$

$$V_{C_L}(t_2) = \frac{1}{C_L} \cdot \int_0^{t_2} A_{I2} \cdot e^{-\alpha_2 \cdot \tau_2} \cdot \sin(\omega_2 \cdot \tau_2) d\tau_2 \tag{3.40}$$

$$V_{C_L}(t_2) = \frac{A_{I2}}{C_L} \cdot \int_0^{t_2} e^{-\alpha_2 \cdot \tau_2} \cdot \sin(\omega_2 \cdot \tau_2) d\tau_2 \tag{3.41}$$

Consider the integral alone:

$$\begin{aligned} & \int_0^{t_2} e^{-\alpha_2 \cdot \tau_2} \cdot \sin(\omega_2 \cdot \tau_2) d\tau_2 \\ = & \frac{-\omega_2 \cdot e^{-\alpha_2 \cdot t_2} \cdot \cos(\omega_2 \cdot t_2) + \alpha_2 \cdot e^{-\alpha_2 \cdot t_2} \cdot \sin(\omega_2 \cdot t_2) - \omega_2}{(\alpha_2^2 + \omega_2^2)} \\ = & \frac{-(e^{-\alpha_2 \cdot t_2} \cdot \omega_2 \cdot \cos(\omega_2 \cdot t_2) + e^{-\alpha_2 \cdot t_2} \cdot \alpha_2 \cdot \sin(\omega_2 \cdot t_2) - \omega_2)}{(\alpha_2^2 + \omega_2^2)} \end{aligned} \tag{3.42}$$

We have: $\omega_2^2 = \omega_{20}^2 - \alpha_2^2$

From Pythagoras'Theorem: $\phi_2 = \arctan(\frac{\alpha_2}{\omega_2})$
Therefore:

$$\begin{aligned} \omega_2 &= \omega_{20} \cdot \cos(\phi_2) \\ \alpha_2 = \omega 20 \cdot \sin(\phi_2) & \\ \omega_{20} = \sqrt{\omega_2^2 + \alpha_2^2} & \end{aligned}$$

Reducing equation 3.42 to:

$$\begin{gathered} \frac{-(e^{-\alpha_2 \cdot t_2} \cdot \omega_{20} \cdot \cos(\phi_2) \cdot \cos(\omega_2 \cdot t_2) + e^{-\alpha_2 \cdot t_2} \cdot \omega_{20} \cdot \sin(\phi_2) \cdot \sin(\omega_2 \cdot t_2) - \omega_2)}{\omega_{20}^2} \\ or \\ \frac{-[e^{-\alpha_2 \cdot t_2} \cdot \omega_{20} (\cdot \cos(\phi_2) \cdot \cos(\omega_2 \cdot t_2) + \sin(\phi_2) \cdot \sin(\omega_2 \cdot t_2)) - \omega_2]}{\omega_{20}^2} \\ or \\ -\frac{e^{-\alpha_2 \cdot t_2} \cdot \omega_{20} \cdot \cos(\omega_2 \cdot t_2 - \phi_2) - \omega_2}{\omega 20^2} \end{gathered} \tag{3.43}$$

Because $\alpha_2 = 0Hz$ gives that $\omega_{20} = \omega_2$ this will result in that equation 3.44 can be written as follows:

$$-\frac{\omega_2 \cdot \cos(\omega_2 \cdot t_2) - \omega_2}{\omega_2^2} \tag{3.44}$$

V_{C_L} is already precharged to $V_{C_L}(0)(= Vdc)$ and can only discharge during state 2. The complete equation for the voltages on the capacitors can be written as a combination of the initial value V_{C_L} with equation 3.44 subtracted: $V_{C_L}(t_2)$:

$$V_{C_L}(t_2) = V_{C_L}(0) + \frac{A_{I2}}{C_L} \cdot \frac{\omega_2 \cdot \cos(\omega_2 \cdot t_2) - \omega_2}{\omega_2^2} \tag{3.45}$$

Due to the fact that the same current is going through C_{Corona}. VC_{Corona} can be derived from equation 3.46.

$$VC_{Corona}(t_2) = -\frac{A_{I2}}{C_{Corona}} \cdot \frac{\omega_2 \cdot \cos(\omega_2 \cdot t_2) - \omega_2}{\omega_2^2} \tag{3.46}$$

The second stage will start when thyristor 2 (Th_2) starts to conduct after V_{C_L} has reached it's maximum. The second stage will stop when the voltage on Th_2 applies with $VTh_2 \leq 0$. The voltage on V_{C_L} will hardly change due to the fact that $C_{Corcona} \ll C_L$, but in the AC/DC/Pulse source there is an extra circuit consisting of a thyristor (Th_3) and a inductance (L_3) which will discharge C_L back to zero before it starts with state 1 again.

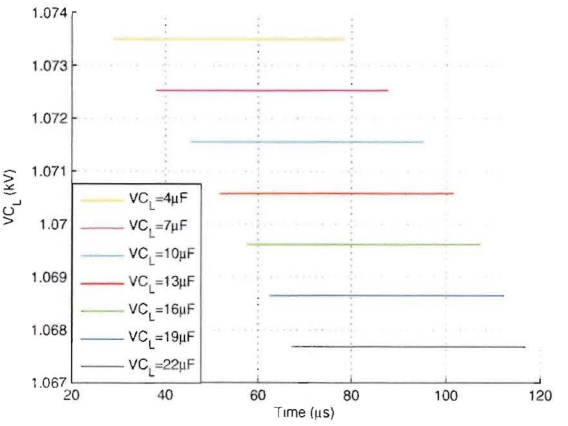

Figure 3.4: Plot of second stage of V_{C_L} model

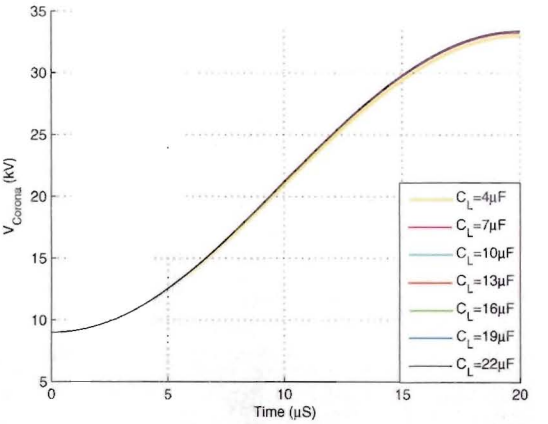

Figure 3.5: Plot of second stage of V_{Corona} model

3.4 Discharging Corona

For the charging part the corona reactor is assumed to have the same characteristics as a capacitor. For the discharging of the corona reactor, the corona reactor is assumed to be a RC-network. This leads to the next model:

$$V_{Corona}(t) = (V_{Corona}max - V_{dc}Corona) \cdot e^{-R_{Corona} \cdot C_{Corona} \cdot t} \quad (3.47)$$

With:

$V_{Corona}max$ = the maximum voltage on the corona reactor after charging.

$V_{dc}Corona$ = the DC-voltage that remains on the corona reactor

R_{Corona} = the resistance value of the corona reactor which get bigger during discharging

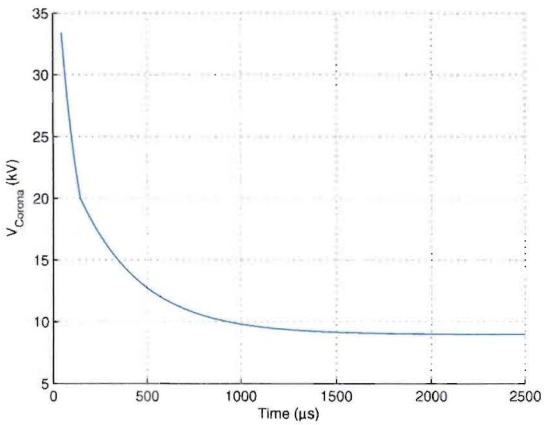

Figure 3.6: Plot of discharging the corona reactor

At $V_{Corona} = 20kV$ there is a dent in the time-resolved waveform, at this point the resistance value of the corona reactor changes to a bigger value. In realtime the dent is not noticeable because it goes more gradually.

3.5 Magnetic pulse compression

Saturable magnetic components have a B-H curve (see fig. 3.8) which is different for each material. For the magnetic pulse compression (mpc) we use saturable magnetic material to compress the pulse. The switching element is the magnetic core which switches the current I. The number of windings is given by N, le is the core magnetic path and Ae is the core cross-section. The specifications of the magnetic material is given in table 3.1.

Table 3.1: Specifications of magnetic material [5]

Magnetic material	Ferrite (Toroid) CMD 5005
Initial permeability	1600
Maximum permeability μ_{max}	4500
Maximum flux density B_{max}	0.3 Tesla
Curie temperature	130^oC
DC volume resistivity	$10^9\Omega - cm$
Blocked voltage	40-50 kV
Inner diameter	90.0 mm
Outer diameter	165.0 mm
Height	49.3 mm
Mean magnetic length	400.5 mm
Cross section	18.48 cm^2
Flux ration $k_B = \frac{B}{B_{max}}$	0.3
Gap distance	$\sim 0.75mm$ Two gaps
Effective permeability	~ 537
Total number of cores	20
High-voltage pulse duration	$\leq 150ns$
Secondary mode impedance	$\sim 840\Omega$
High voltage capacitor	$\leq 30nF$
Maximum average power at 1000 pps and the referred output voltage	24 kW at 80 kV

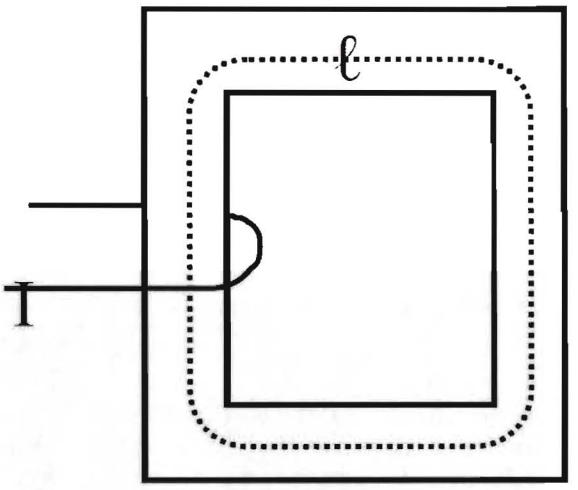

Figure 3.7: Model of the saturable inductor

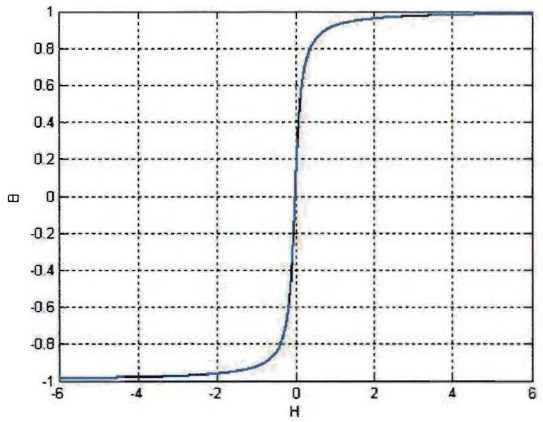

Figure 3.8: B-H curve of a saturable magnetic material

$$H = \frac{N \cdot I}{l_e} \tag{3.48}$$

$$B = \mu_r \cdot \mu_0 \cdot \frac{N \cdot I}{l_e} \tag{3.49}$$

$$\frac{B}{H} = \mu_r \cdot \mu_0 \tag{3.50}$$

$$L = \frac{d}{dH} B \cdot \frac{N^2 \cdot A_e}{l_e} = \mu_r \cdot \mu_0 \cdot \frac{N^2 \cdot A_e}{l_e} \tag{3.51}$$

For the saturable inductor used for the magnetic pulse compression this leads to:

$$N = 123$$

$$\frac{B_{sat}}{H_{sat}} = \mu_r \cdot \mu_0 \approx 1$$

$$I_{sat} = \frac{B_{sat} \cdot l_e}{\mu_r \cdot \mu_0 \cdot N} \approx 1mA$$

The traditional magnetic pulse compression network consist of two capacitors and a saturable inductor (see fig.3.9).

In this project the corona reactor is split in two parts and replaces the two capacitors. The behavior of the corona reactors are the same as that of a capacitor. The network can be drawn as follows: (see fig.3.10)[1]

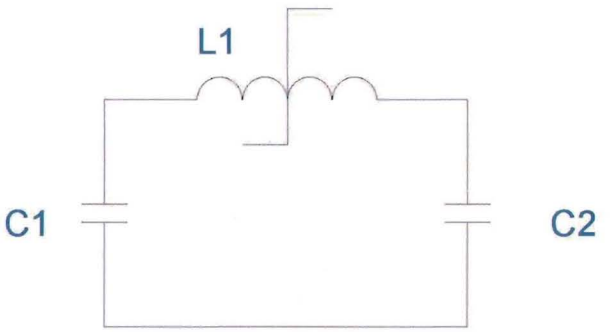

Figure 3.9: Traditional magnetic pulse compression network

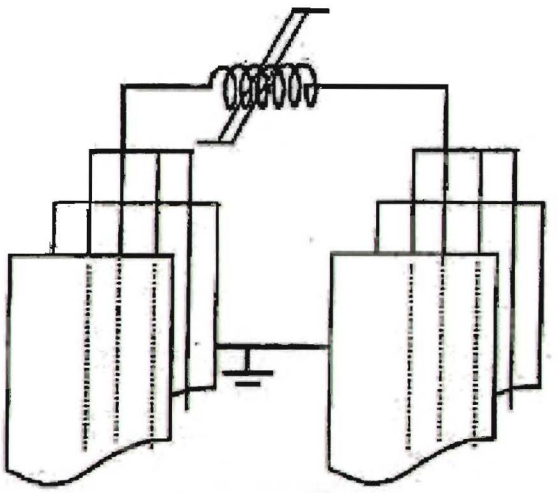

Figure 3.10: Magnetic pulse compression with two compartment mpc corona reactor

For the model there doesn't change much, because with saturation the only thing that differs is the value of the saturable inductor. If we reckon this the model needs to adjust the inductance value during the process which is about the same as with the discharging part of the corona reactor. This gives the next plot (see fig.3.11) where the value of the inductor decreases about ten times.

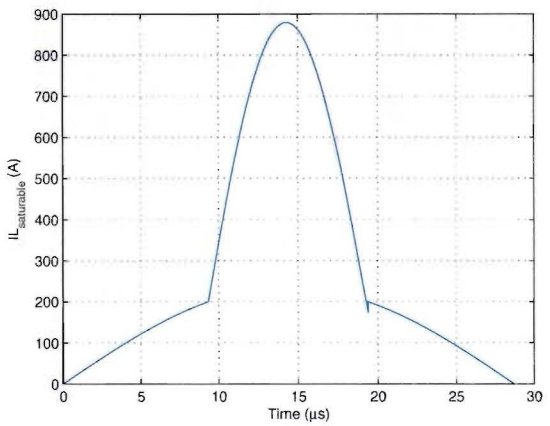

Figure 3.11: Current through the saturable inductor

3.6 Matching

For an AC/DC/Pulse source combined with a corona reactor the matching between the source capacitor and the corona reactor is expected that it has to be ideal. The ideal value can be calculated with the energy equation of an ideal transformer and with formula 3.52.

$$C_L = N^2 \cdot C_{Corona} \tag{3.52}$$

Due to the fact that there is a remaining Voltage on the corona reactor, V_{dc}, formula 3.52 needed to be adjusted to formule 3.53, with E_1 the primary energy, E_2 the secondary energy, V_0 the primary voltage, the output from low voltage part or input to the transformer, V_{DC} secondary DC-voltage, V_p secondary

peak voltage and C_{Corona} the corona reactor capacitance:

$$\begin{aligned}
E_1 &= E_2 \\
\frac{1}{2} \cdot C_L \cdot V_0^2 &= \frac{1}{2} \cdot C_{Corona} \cdot (V_p^2 - V_{dc}^2) \\
C_L \cdot V_0^2 &= C_{Corona} \cdot (V_p^2 - V_{dc}^2) \\
N \cdot V_0 &= V_p + V_{dc} \\
C_L \cdot \frac{(V_p + V_{dc})^2}{N^2} &= C_{Corona} \cdot (V_p^2 - V_{dc}^2) \\
C_L &= N^2 \cdot C_{Corona} \cdot \frac{(V_p^2 - V_{dc}^2)}{(V_p + V_{dc})^2} \\
V_p^2 - V_{dc}^2 &= (V_p + V_{dc})(V_p - V_{dc}) \\
C_L &= N^2 \cdot C_{Corona} \cdot \left(\frac{V_p - V_{dc}}{V_p + V_{dc}}\right) \\
C_L &= N^2 \cdot C_{Corona} \cdot \left(1 - \frac{2 \cdot V_{dc}}{N \cdot V_0}\right) \quad (3.53) \\
\text{This can also be written as: } C_L &= N^2 \cdot C_{Corona} \cdot \left(\frac{2 \cdot V_p}{N \cdot V_0} - 1\right) \quad (3.54)
\end{aligned}$$

This formula is given by Sreejit [7][8], but in this model it is expected that V_0 fully discharges and as shown in figure 4.1 this doesn't happen. When the transformer ratio is big enough this wouldn't happen, but in this case (N=36) V_0 doesn't fully discharge to zero and has a remaining DC-voltage. Due to this the calculated value for C_L can't be correct. For example if equation 3.53 is used for a corona reactor plate distance of 9 cm, there is a deficiency with the measurement.

$$\begin{aligned}
&D = 9cm && V_0 = 1.074kV && C_{Corona} = 250pF \\
&N \cdot V_0 = V_p + V_{dc} \quad \Rightarrow && V_{dc} = 8.9813kV && V_p = 29.6827kV
\end{aligned}$$

$$C_L = (36)^2 \cdot 250 \cdot 10^{-12} \left(1 - \frac{2 \cdot 8.9813 \cdot 10^3}{36 \cdot 1.074 \cdot 10^3}\right)$$

$$C_L = 1.73 \cdot 10^{-7}$$

With the next calculations the V_{dc} on the primary side isn't neglected. V_0 will be replaced by $V_{P_{primary}}$ and with the use of formula 3.54 instead of formula 3.53 this results in:

$$\begin{aligned}
&D = 9cm && V_{P_{primary}} = 120V && C_{Corona} = 250pF \\
&N \cdot V_0 = V_p + V_{dc} \quad \Rightarrow && V_{dc} = 8.9813kV && V_p = 23.02kV
\end{aligned}$$

$$C_L = (36)^2 \cdot 250 \cdot 10^{-12} \left(\frac{2 \cdot 23.02 \cdot 10^3}{36 \cdot 120} - 1\right)$$

$$C_L = 3.129 \cdot 10^{-6}$$

Table 3.2: $C_{L_{matched}}$ for different plate distances

D	V_p	C_{Corona}	$C_{L_{matched}}$
9 cm	23.02 kV	250 pF	$3.129\mu F$
10 cm	25.1 kV	243 pF	$3.344\mu F$
11 cm	25.0 kV	234 pF	$3.207\mu F$

This is a better approach of the matched value, but for bigger plate distances the capacitance value of the corona reactor decreases and the voltages hardly changes (see table 3.2). Thus the problem of the remaining DC-voltage on V_{C_L} only increases (see figure 4.31). As the measurements show (see figure 4.24) the matched values for C_L aren't reached for $D > 9cm$. $C_L matched$ for the 10 cm and 11 cm setup is probably $C_L matched > 22\mu F$. Thus formula 3.53 nor formula 3.54 nor formula 3.52 is suitable for calculating the matched value $C_L matched$.

Chapter 4

Experimental test results

4.1 Typical waveforms

Figure 4.1 shows a typical time-resolved voltage waveform of C_L. Figure 4.2 shows a typical time-resolved voltage waveform at the primary side of the AC/DC/Pulse source, and figure 4.3 shows the corresponding current at the primary side of the AC/DC/Pulse source. The typical power obtained after multiplying the voltage and current on the primary side and after time-integrating the power the energy are respectively shown in figure 4.4 and figure 4.5. Figure 4.6, figure 4.7, figure 4.8 and figure 4.9 show respectively the typical high-voltage and current on the corona reactor, the corona power and the corona energy. The corona reactor contains one compartment and the settings for the typical waveforms are: $C_L = 22\mu F$ and $C_{Corona} = 230 \sim 243pF$.

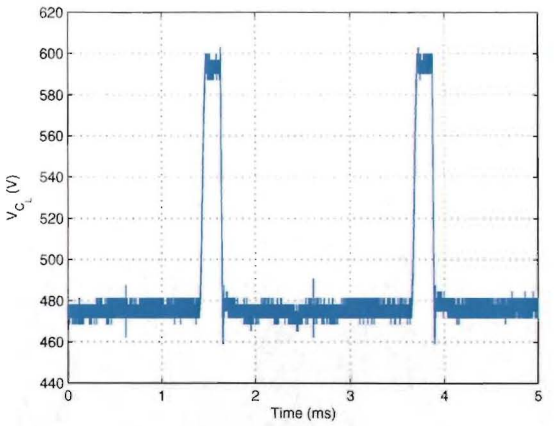

Figure 4.1: Typical voltage C_L

As shown in figure 4.1 the voltage V_{C_L} doesn't go below zero, this means that Th_3 (see figure 2.1) will never be switched on thus redundant.

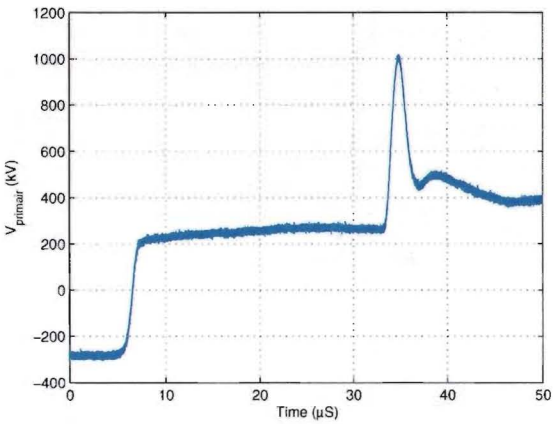

Figure 4.2: Typical voltage at primary side of the AC/DC/Pulse source

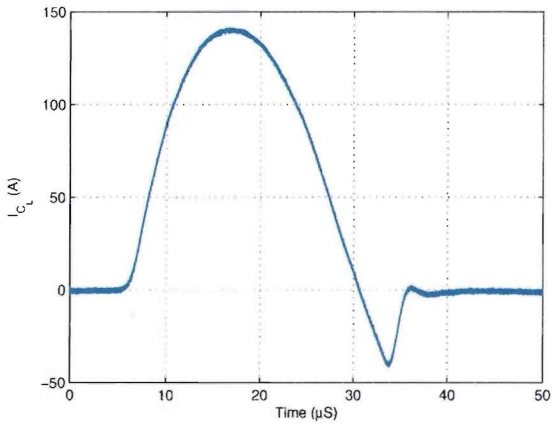

Figure 4.3: Typical current at primary side of the AC/DC/Pulse source

The negative peak current in figure 4.3 is caused by the recovery charge of the thyristor Th_2 (see table: 2.1) which is between $350\mu C$ and $560\mu C$. This explains also the high peak in figure 4.2 which occurs at the same time. This is caused due to the fact that the measurements on the primary side of the transformer (TR) are done differentially also after opening Th_2 the circuit is open and there starts an oscillation on the primary side determined by circuit C_L-L_2-TR-R_5-D_2 and the parasitic capacitance of TR. These oscillating peaks are neglected for the calculations of the energy because the energy to the corona reactor isn't influenced by these oscillations.

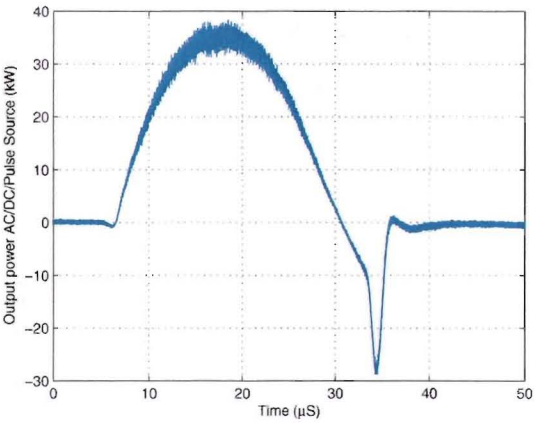

Figure 4.4: Typical power at the primary side of the AC/DC/Pulse source obtained after multiplying $V_{primary}$ (figure 4.2) and I_{C_L} (figure 4.3)

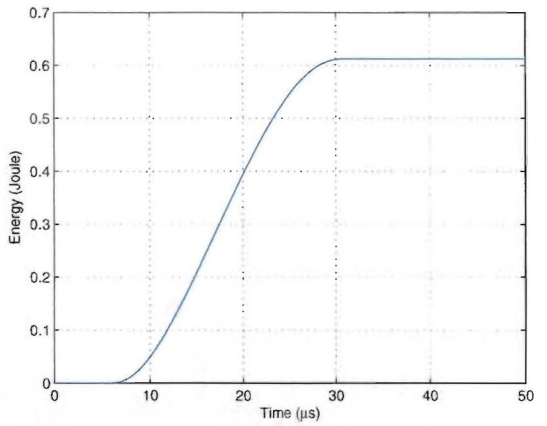

Figure 4.5: Typical energy at the primary side of the AC/DC/Pulse source obtained after time-integrating the power at the primary side of the AC/DC/Pulse source (figure 4.4)

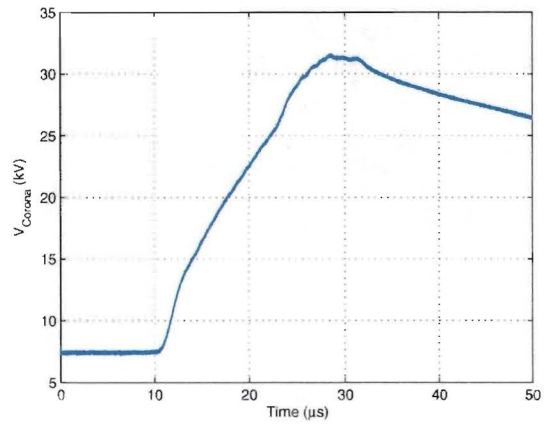

Figure 4.6: Typical voltage on the corona reactor

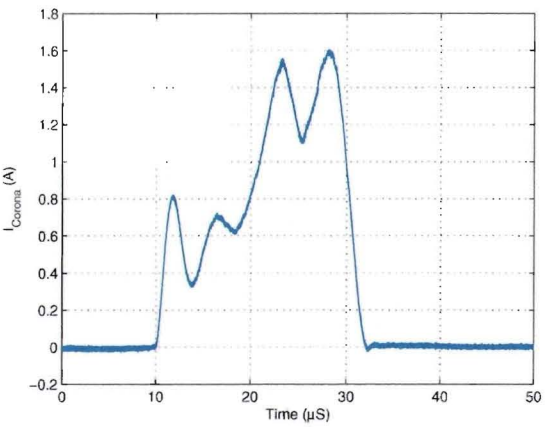

Figure 4.7: Typical corona reactor current

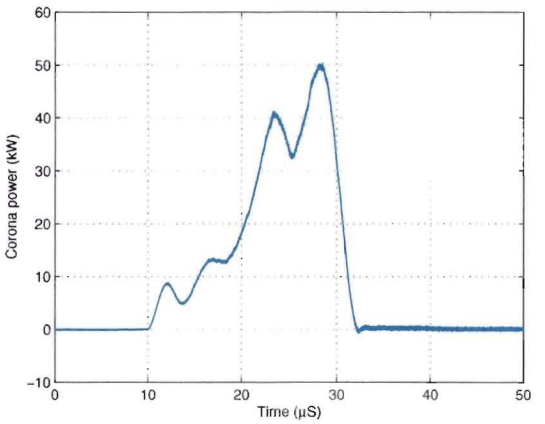

Figure 4.8: Typical corona power of the AC/DC/Pulse source obtained after multiplying V_{Corona} (figure 4.2) and I_{Corona} (figure 4.7)

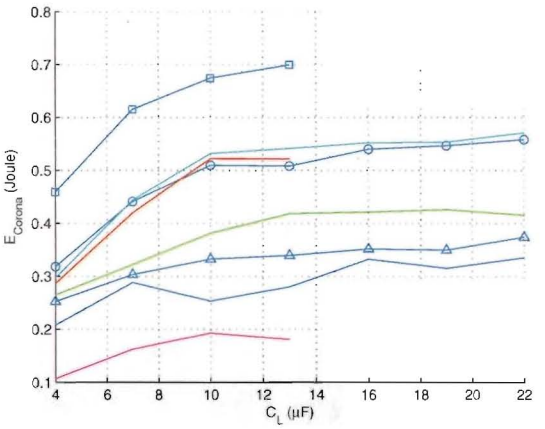

Figure 4.9: Typical corona energy of the AC/DC/Pulse source obtained after time-integrating the corona power of the AC/DC/Pulse source (figure 4.8)

Figure 4.10 shows charging and discharging pulses at the primary side of the AC/DC/Pulse source with a pulse repetition rate of 446 pps. Figure 4.11 and figure 4.12 show respectively the voltage and current on the corona reactor with a pulse repetition rate of 446 pps.

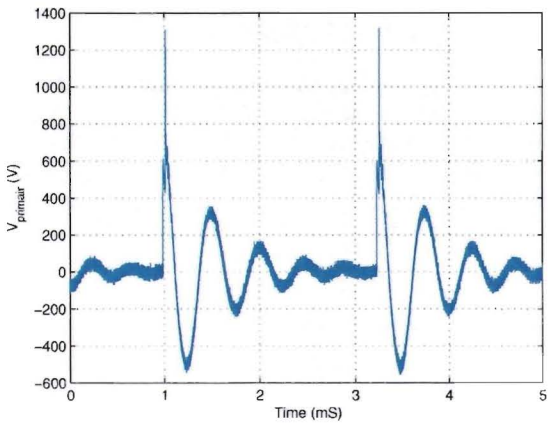

Figure 4.10: Typical voltage on the primary side of the AC/DC/Pulse source with a repetition rate of 446 pps

As already stated in figure 4.2 after switching Th_2 the voltage on the primary side of transformer TH starts to oscillate, this oscillation causes an extra peak in V_{Corona} (see figure 4.11). This extra peak doesn't influence the calculations of the energy or other calculations because the current (I_{Corona}) during this peak is hardly evident. [9]

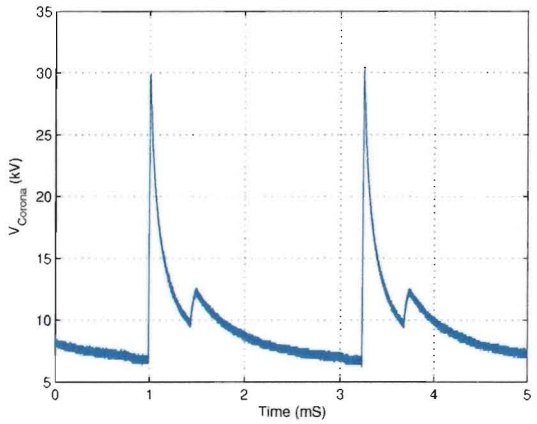

Figure 4.11: Typical voltage on the corona reactor with a pulse repetition rate of 446 pps

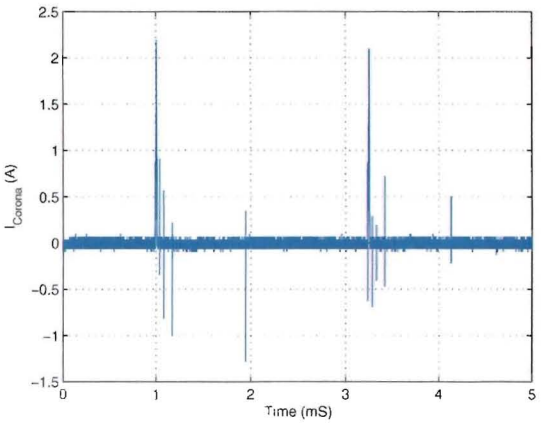

Figure 4.12: Typical corona reactor current with a pulse repetition rate of 446 pps

4.2 One compartment corona reactor

4.2.1 Plate distance 9 cm

The average flow during the measurements with a distance between the plates of 9 centimeters was 1.83 m/s. With a deviation of 0.01 m/s it is acceptable to use the average value for further calculations. The humidity during the measurements was 57% and the temperature was 22°C. The small plate distance between the two plates limited the size of the capacitor value C_L to $C_L \leq 13\mu F$, higher values of C_L would cause to many breakthroughs to get reliable measurements. The value of the capacitance of the corona reactor varies between $240 \sim 250pF$.

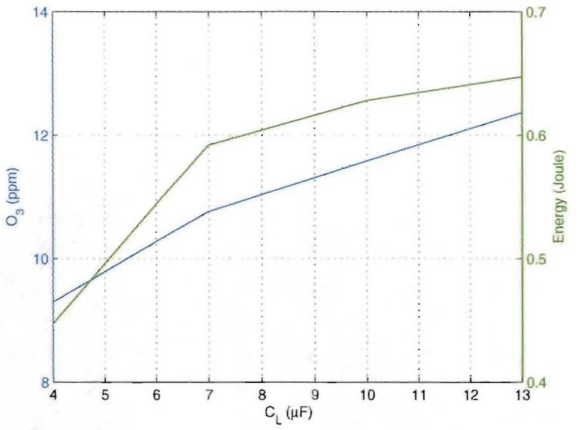

Figure 4.13: Corona energy and Ozone production 9 cm

For the calculation of the ozone production equation 4.1 is used.

$$\begin{aligned} Ozoneproduction &= Measurements \times \rho \times 1000 \\ Ozoneproduction &= [ppm] \\ Measurements &= [mol/m^3] \\ \rho &= \frac{m}{V} = 0,002144 \frac{g}{cm^3} \end{aligned} \tag{4.1}$$

In figure 4.13 the results of the measurements of the energy consumption and the ozone production are given with on the right y-axis the energy $[Joule]$ and on the left y-axis the ozone concentration $[ppm]$ against the capacitance value C_L. The energy values are obtained after multiplying the corona reactor voltage and current and time-integrating them. The current also contains the displacement current which doesn't contribute to the total energy in the corona reactor, the amount of the displacement current is really small, less then 1%, so it's negligible.

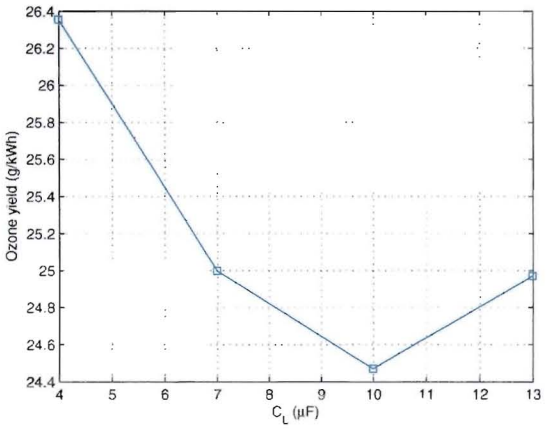

Figure 4.14: Ozone yield 9 cm

Figure 4.14 shows that the ozone yield for the various values of C_L differ slightly. Also in figure 4.13 the difference between the ozone concentrations of the produced ozone and the average energy per pulse doesn't differ that much. The expectation was that the ozone yield would form a straight line, but due to the fact that a small change in energy has already a big influence on the ozone yield as is shown in formula 4.2 this couldn't be realized for these measurements.

$$\begin{aligned} Ozoneyield &= \frac{Measurements \times M \times V \times 1000}{P_{plasma}} \\ Measurements &= [mol/m^3] \\ M &= molecular\ mass[g/mol] \\ V &= flow[m^3/h] \\ P_{plasma} &= energy\ per\ pulse\ [J] \times rep\ rate\ [s^{-1}] \\ Ozoneyield &= [g/kWh] \end{aligned} \tag{4.2}$$

4.2.2 Plate distance 10 cm

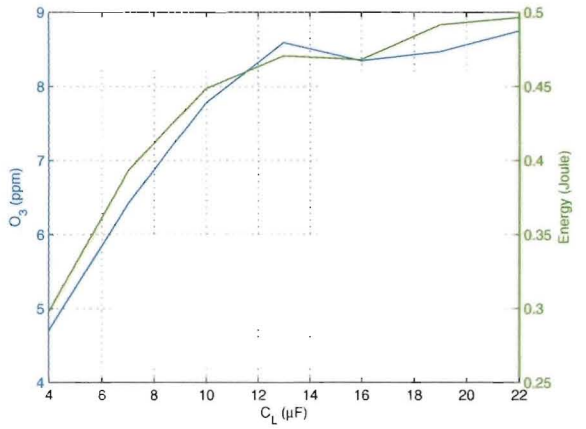

Figure 4.15: Corona energy and Ozone production 10 cm

The average flow during the measurements with a distance between the plates of 10 centimeters was 1.87 m/s. With a deviation of 0.02 m/s it is acceptable to use the average value for further calculations. The humidity during the measurements was 57% and the temperature was 22°C. During the measurements breakthroughs were only occurring with a $C_L > 16\mu F$ but were still rarely and didn't influence any of the measurement. The size of the C_L was limited by the amount of available capacitors suitable for the AC/DC/Pulse source. The value of the capacitance of the corona reactor varies between $230 \sim 243pF$.

In figure 4.15 the results of the measurements of the energy consumption and the ozone production are given with on the right y-axis the energy $[Joule]$ and on the left y-axis the ozone concentration $[ppm]$ against the capacitance value C_L. The energy values are obtained after multiplying the corona reactor voltage and current and time-integrating them. The corona reactor current also contains the displacement current which doesn't contribute to the total energy in the corona reactor, the amount of the displacement current is really small, less then 1%, so it's negligible.

Figure 4.16 shows that the ozone yield for the various values of C_L differ slightly. In figure 4.15 the difference between the ozone concentration of the produced ozone and the average energy per pulse also doesn't differ that much. The expectation was that the ozone yield would form a straight line, but due to the fact that a small change in energy has already a big influence on the ozone yield as is shown in formula 4.2 this couldn't be realized for these measurements.

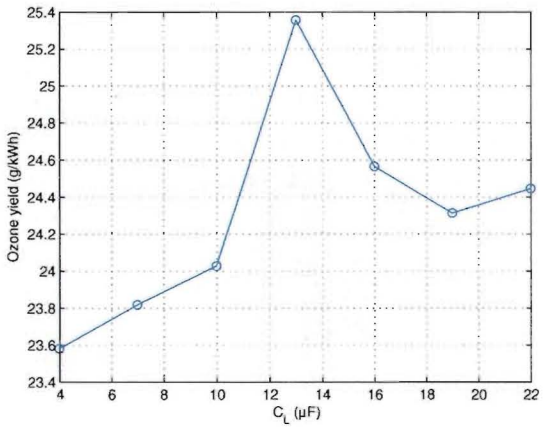

Figure 4.16: Ozone yield 10 cm

4.2.3 Plate distance 11 cm

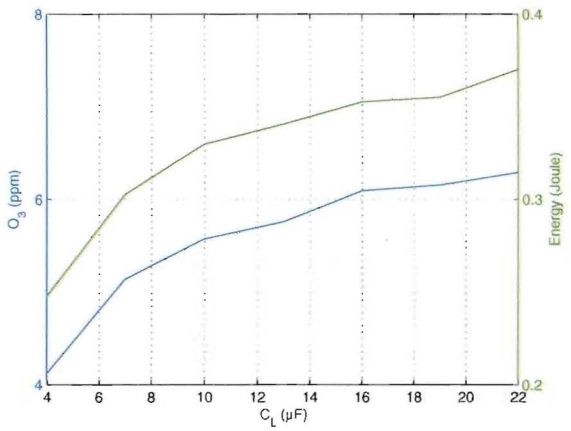

Figure 4.17: Corona energy and Ozone production 11 cm

The average flow during the measurements with a distance between the plates of 11 centimeters was 1.84 m/s. With a deviation of 0.02 m/s it is acceptable to use the average value for further calculations. The humidity during the measurements was 57% and the temperature was 22°C. During the measurements breakthroughs were only occurring with a $C_L > 19\mu F$ but were still rarely and didn't influence any of the measurement. The size of the C_L was limited by the amount of available capacitors suitable for the AC/DC/Pulse source. The value of the capacitance of the corona reactor varies between $225 \sim 234pF$.

In figure 4.17 the results of the measurements of the energy consumption and the ozone production are given with on the right y-axis the energy $[Joule]$ and on the left y-axis the ozone concentration $[ppm]$ against the capacitance value

C_L. The energy values are obtained after multiplying the corona reactor voltage and current and time-integrating them. The corona reactor current also contains the displacement current which doesn't contribute to the total energy in the corona reactor, the amount of the displacement current is really small, less than 1%, so it's negligible.

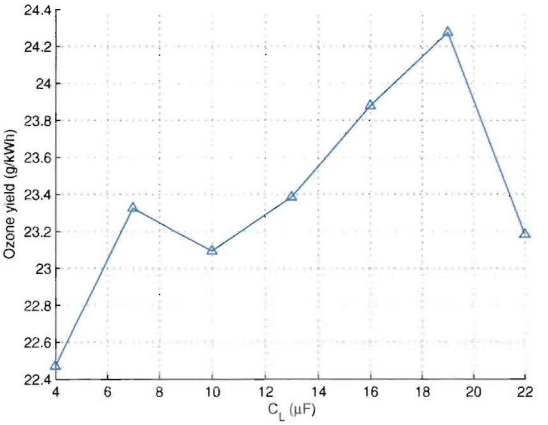

Figure 4.18: Ozone yield 11 cm

Figure 4.18 shows that the ozone yield for the various values of C_L differ slightly. In figure 4.17 the difference between the ozone concentration of the produced ozone and the average energy per pulse also doesn't differ that much. The expectation was that the ozone yield would form a straight line, but due to the fact that a small change in energy has already a big influence on the ozone yield as is shown in formula 4.2 this couldn't be realized for these measurements.

4.3 Two compartment corona reactor

Figure 4.19 and figure 4.20 shows the corona reactor with indicated the numbers of each compartment. Because there are two compartments the total capacitance value of the two compartment corona reactor is bigger. This means that the expression $C_L \gg C_{Corona}$ isn't valid anymore, but $C_L > C_{Corona}$ is. Due to this the voltage on C_L changes during the charging part of C_{Corona} as shown in figure 4.21. But this only happens with a small C_L ($C_L < 13\mu F$).

The current in compartment 1 of the two compartment corona reactor has the same waveform as the typical waveform at the primary side of the one compartment corona reactor (shown in figure 4.3). Also the voltage on the two compartment corona reactor and the current are the same as the typical waveforms of chapter 4.1.

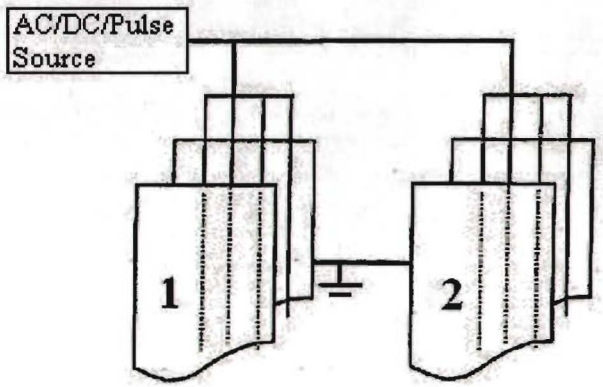

Figure 4.19: The two compartments where compartment 1 of the corona reactor is indicated with **1** and compartment 2 of the corona reactor is indicated with **2**

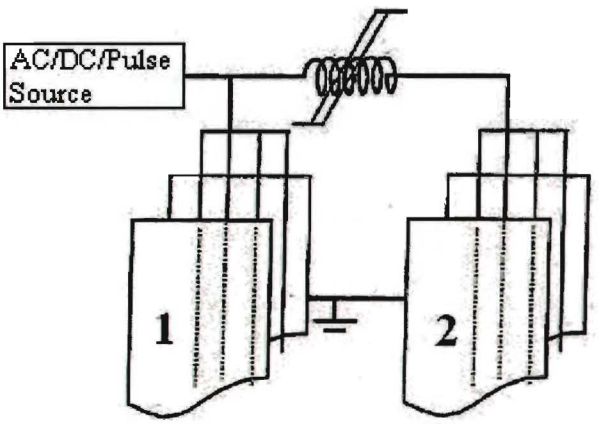

Figure 4.20: Magnetic pulse compression with two compartments where compartment 1 of the mpc corona reactor is indicated with **1** and compartment 2 of the corona reactor is indicated with **2**

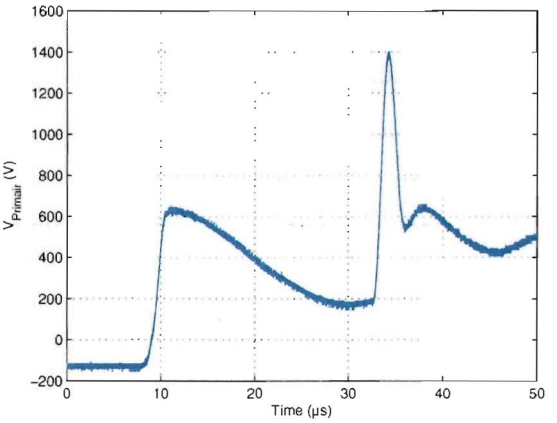

Figure 4.21: Voltage at the primary side of the two compartment corona reactor with $C_L = 4\mu F$

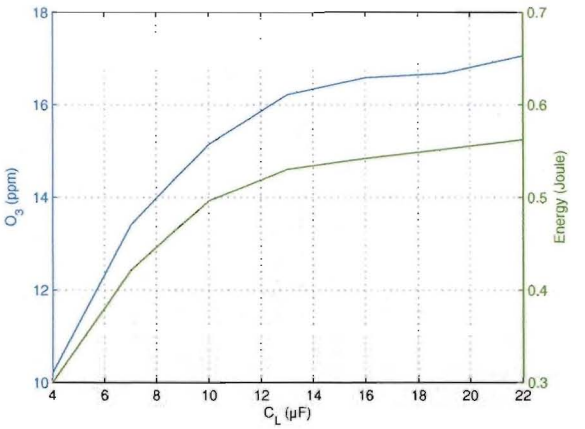

Figure 4.22: Total energy in the two compartment corona reactor 10-10cm and total Ozone production

The average flow during the measurements with the two compartment corona reactor was 1.77 m/s. Due to a small deviation of the flow between the measurements it's acceptable to use the average value for further calculations. The humidity during the measurements was 49.9% and the temperature was 22°C. During the measurements breakthroughs were only occurring with a $C_L > 19\mu F$ but were still rarely and didn't influence any of the measurements. The size of C_L was limited by the amount of available capacitors suitable for the AC/DC/Pulse source. The value of the total capacitance of the two compartment corona reactor 10-10 cm varies between $539 \sim 548pF$.

In figure 4.22 the results of the measurements of the energy consumption and the ozone production are given with on the right y-axis the energy $[Joule]$ and on the left y-axis the ozone concentration $[ppm]$ against the capacitance value C_L. The energy values are obtained after multiplying the corona reactor voltage and current and time-integrating them. The corona reactor current also contains the displacement current which doesn't contribute to the total energy in the corona reactor, the amount of the displacement current is really small, less than 1%, so it's negligible.

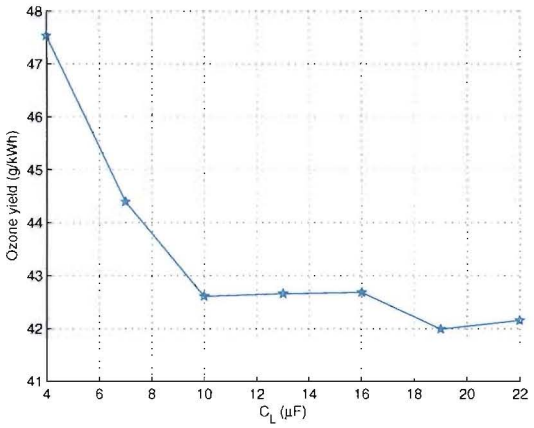

Figure 4.23: Ozone yield of the two compartment corona reactor 10-10 cm

Figure 4.23 shows that the ozone yield for $C_L < 10\mu F$ differ quit a lot but in figure 4.22 the difference between the ozone concentration of the produced ozone and the average energy per pulse doesn't differ that much. The expectation was that the ozone yield would form a straight line, but due to the fact that a small change in energy has already a big influence on the ozone yield as is shown in formula 4.2 this couldn't be realized for these measurements.

4.4 Efficiency

The ratio of energy subtracted from C_L and the energy dissipated in the corona reactor is defined to be the efficiency. For the calculation of the efficiency only the change in voltage and current is used. This means that the DC-value of the primary AC/DC/Pulse source and V_{Corona} are ignored (see Appendix B). For the one compartment corona reactor the efficiency and energy are equivalent (see figure 4.9). But as shown in figure 4.33 the efficiency isn't depending on the voltage because in that figure the 9 cm setup has the lowest voltage and the 11 cm the highest. Thus the efficiency is depending on the current which is supported by figure 4.28 where 9 cm does indeed have the highest value.

The two compartment corona reactor and mpc corona reactor both have a better efficiency. This is due to the better matching since the capacitance of both two compartment corona reactors is bigger than the capacitance of the one compartment corona reactor thus the energy transfer is better (see formula 4.3).

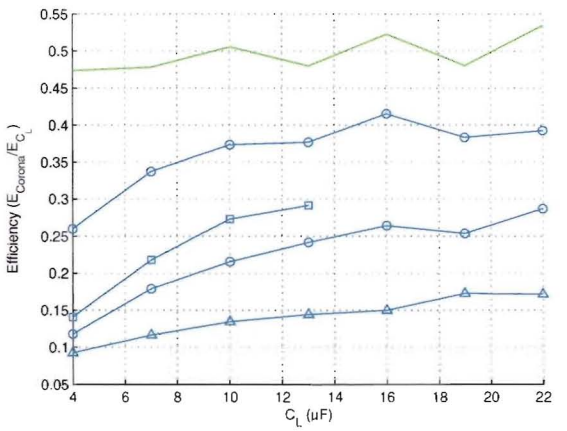

Figure 4.24: Efficiency of the one compartment corona reactor with: □: 9cm, ○: 10cm, △: 11cm, the two compartment corona reactor with: ⋆: 10-10 cm and the two compartment mpc corona reactor: Green: 10-10 cm

4.5 Two compartment mpc corona reactor

To make clear what is mend with compartment 1 and compartment 2 of the two compartment mpc corona reactor figure 4.20 shows the two compartment mpc corona reactor.

To compare the results of the one compartment corona reactor, the two compartment corona reactor with the two compartment mpc corona reactor, the results of the one compartment corona reactor as discussed in chapter 4.2.1, chapter 4.2.2 and 4.2.3 and the results of the two compartment corona reactor as discussed in chapter 4.3 will also be plotted in the figures but dotted.

4.5.1 Energy

Figure 4.25 shows the total energy to the corona reactor. The measurements show that the energy of the two compartment mpc corona reactors is about twice the energy as the same plate distance one compartment corona reactor. For the two compartment corona reactor 10-10 cm there is no difference in total energy with the one compartment corona reactor 10 cm.

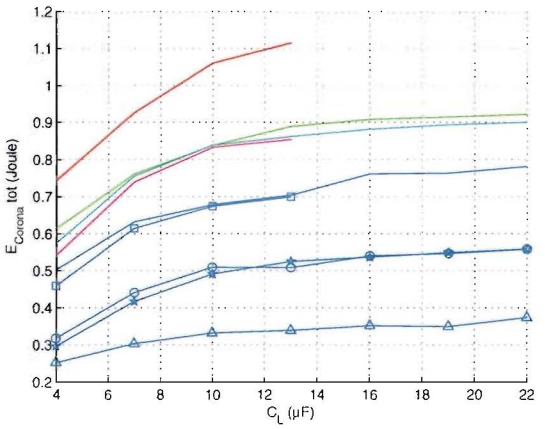

Figure 4.25: Total energy of the two compartment mpc corona reactor with: Red: 9-9cm, Green: 10-10cm, Blue: 11-11cm, Cyan: 9-11cm and Magenta: 11-9cm, the two compartment corona reactor with: $\star$: 10-10 cm and the one compartment corona reactor with: $\square$: 9cm, $\bigcirc$: 10cm, $\triangle$: 11cm

Figure 4.26 shows the energy in compartment 1 of two compartment corona reactor and mpc corona reactor. The measurements show that there is hardly any difference between compartment 1 of the two compartment mpc corona reactors 9-9 cm, 9-11 cm and the one compartment corona reactor 10 cm. These minimal difference can be explained by the fact that the total impedance of the two compartment mpc corona reactor doesn't differ much compared to total impedance of the one compartment corona reactor (see equation 4.3).

$$\begin{aligned} \frac{1}{Z_{Corona}} &= C_{Cell_1} + \frac{1}{L_{saturable}} + C_{Cell_2} \\ Z_{Corona} &= \frac{L_{saturable}}{(C_{Cell_1} + C_{Cell_2}) \cdot L_{saturable} + 1} \end{aligned} \tag{4.3}$$

This applies also for the two compartment mpc corona reactors 10-10 cm, 11-11 cm and the one compartment corona reactor 11 cm but the mutually deviation is bigger then with the two compartment mpc corona reactors 9-9 cm, 9-11 cm and the one compartment corona reactor 10 cm. This can be explained with the fact that if the plate distance is longer the corona intension is less intensive and stable.

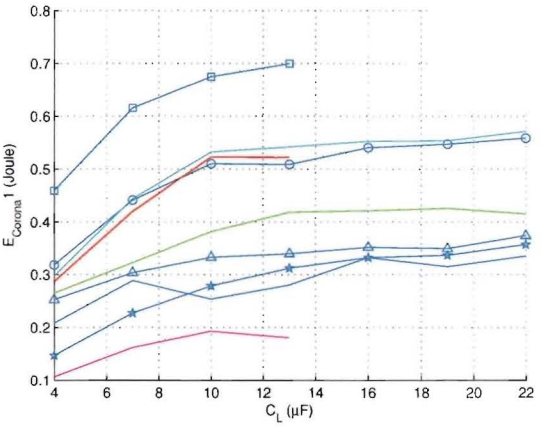

Figure 4.26: Energy in compartment 1 of the mpc corona reactor with: Red: 9-9cm, Green: 10-10cm, Blue: 11-11cm, Cyan: 9-11cm and Magenta: 11-9cm, the two compartment corona reactor with: $\star$: 10-10 cm and the one compartment corona reactor with: $\square$: 9cm, $\bigcirc$: 10cm, $\triangle$: 11cm

In figure 4.27 the energy in compartment 2 of the two compartment corona reactor and mpc corona reactor is shown. The energy of compartment 2 of the corona reactor 11-9 cm is about the same as the one compartment corona reactor 9 cm. This explains why the measurements with $C_{I,} > 13\mu F$ of the two compartment mpc corona reactor 9-11 cm were not reliable due to the same problems as with the one compartment corona reactor 9 cm. It is, as shown in figure 4.26, made clear why the energy to compartment 1 of the corona reactor 9-11 cm is much lower ($C_{11} \ll C_9$). The energy to compartment 1 and compartment 2 of the corona reactors 10-10 cm, 11-11 cm and the one compartment corona reactor 10 cm are also close to each other. Besides that it occurs that compartment 2 of the corona reactors 9-9 cm, 10-10 cm and 11-11 cm get more energy than compartment 1 of these two compartment mpc corona reactors. This can be explained by the fact that compartment 2 of the corona reactor doesn't suffer from any oscillation with the saturable inductor so the voltage (thus the energy) remains higher for a longer time.[10]

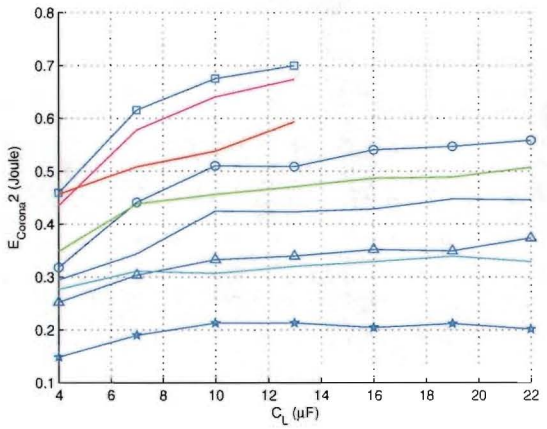

Figure 4.27: Energy in compartment 2 of the mpc corona reactor with: Red: 9-9cm, Green: 10-10cm, Blue: 11-11cm, Cyan: 9-11cm and Magenta: 11-9cm, the two compartment corona reactor with: $\star$: 10-10 cm and the one compartment corona reactor with: $\square$: 9cm, $\bigcirc$: 10cm, $\triangle$: 11cm

4.5.2 Currents and Voltages

In figure 4.28 the maximum current into the corona reactor is made clear. The measurements correspond with the expectations, the currents of the two compartment mpc corona reactors are higher than the one compartment corona reactors except for the two compartment mpc corona reactor 11-11 cm which is corresponding with the one compartment corona reactor 9 cm. The current of the two compartment corona reactor 10-10 cm is higher than the current of the one compartment corona reactor 10 cm, while the energy was about the same. This means that the high-voltage of the two compartment corona reactor 10-10 cm has to be lower than the high-voltage of the one compartment corona reactor 10 cm (see figure 4.33). The current is also an indication of the ozone production which will be discussed in chapter 4.5.3, and explains why the current of the two compartment mpc corona reactor 11-11 cm is about the same as the one compartment corona reactor 9 cm.

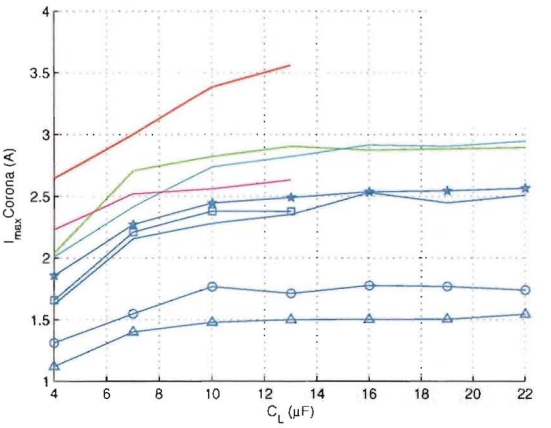

Figure 4.28: Total corona reactor current of the two compartment mpc corona reactor with: Red: 9-9cm, Green: 10-10cm, Blue: 11-11cm, Cyan: 9-11cm and Magenta: 11-9cm, the two compartment corona reactor with: $\star$: 10-10 cm and the one compartment corona reactor with: $\square$: 9cm, $\bigcirc$: 10cm, $\triangle$: 11cm

To see if there are differences between the currents going to each compartment separately of the two compartment corona reactor and the two compartment mpc corona reactor as well as the current going to the one compartment corona reactor, figure 4.29 and figure 4.30 show the current going respectively to compartment 1 and to compartment 2. The difference in current between two equal plate distance compartments of the two compartment corona reactor and mpc corona reactor is minimal, but the differences in currents between two different plate distance compartments of the two compartment mpc corona reactor is much bigger. This is equal to formula 4.4:

$$I = C\frac{\partial V}{\partial t} \tag{4.4}$$

The total voltage (V_C) is constant on the two compartments of the two compartment mpc corona reactor, so the current has to change.

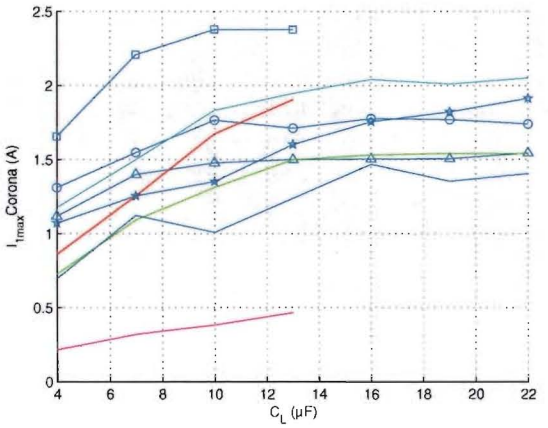

Figure 4.29: Corona reactor current of compartment 1 of the corona reactor with: Red: 9-9cm, Green: 10-10cm, Blue: 11-11cm, Cyan: 9-11cm and Magenta: 11-9cm, the two compartment corona reactor with: ⋆: 10-10 cm and the one compartment corona reactor with: □: 9cm, ◯: 10cm, △: 11cm

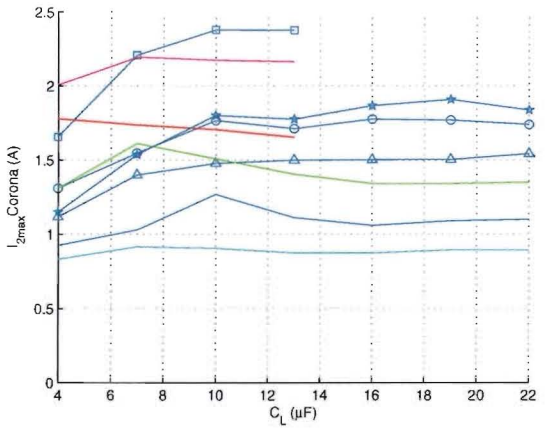

Figure 4.30: Corona reactor current of compartment 2 of the corona reactor with: Red: 9-9cm, Green: 10-10cm, Blue: 11-11cm, Cyan: 9-11cm and Magenta: 11-9cm, the two compartment corona reactor with: ⋆: 10-10 cm and the one compartment corona reactor with: □: 9cm, ◯: 10cm, △: 11cm

The sizes of the capacitance value of the two compartment mpc corona reactors are bigger than the one compartment corona reactors. This explains the differences in V_{dc} between the different plate distances in figure 4.31, as the capacitive value of the compartment(s) of the corona reactor increases $V_{dc}max$ will decrease. Another phenomenon is that the peaks correspond with the peaks in figure 4.32, if there is a peak in the $V_{dc}max$ there is a corresponding peak in the V_pmax so that $V_{corona}max$ is about the same as with an other value of C_L. The $V_{Corona}max$ (see figure 4.33) of the two compartment mpc corona reactors are lower than the one compartment corona reactors. This is logic due to the fact that the total currents (see figure 4.28) of the two compartment mpc corona reactors is higher then the currents of the one compartment corona reactors.

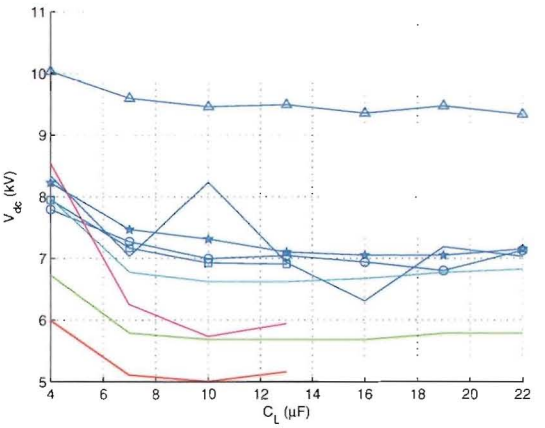

Figure 4.31: Initial DC voltage on the two compartment mpc corona reactor with: Red: 9-9cm, Green: 10-10cm, Blue: 11-11cm, Cyan: 9-11cm and Magenta: 11-9cm, the two compartment corona reactor with: $\star$: 10-10 cm and the one compartment corona reactor with: $\square$: 9cm, $\bigcirc$: 10cm, $\triangle$: 11cm

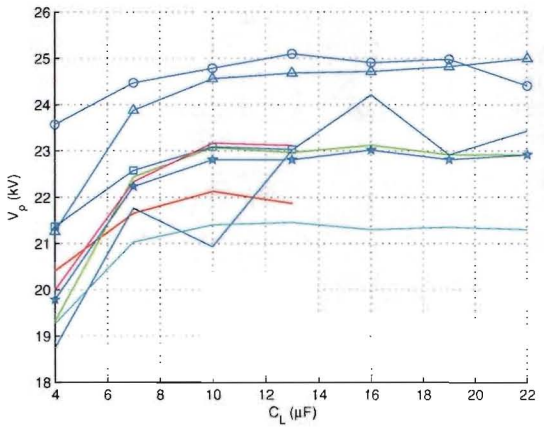

Figure 4.32: Peak voltage on the two compartment mpc corona reactor with: Red: 9-9cm, Green: 10-10cm, Blue: 11-11cm, Cyan: 9-11cm and Magenta: 11-9cm, the two compartment corona reactor with: ⋆: 10-10 cm and the one compartment corona reactor with: □: 9cm, ◯: 10cm, △: 11cm,

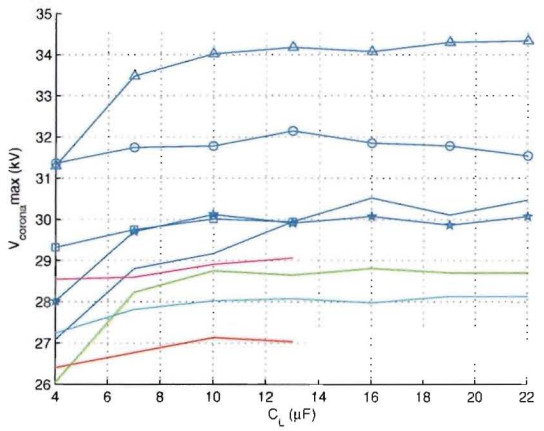

Figure 4.33: Total voltage on the two compartment mpc corona reactor with: Red: 9-9cm, Green: 10-10cm, Blue: 11-11cm, Cyan: 9-11cm and Magenta: 11-9cm, the two compartment corona reactor with: ⋆: 10-10 cm and the one compartment corona reactor with: □: 9cm, ◯: 10cm, △: 11cm

But the most important difference between the two compartment corona reactor and the two compartment mpc corona reactor is the pulse duration. As shown in figure 4.34 the pulse rise time is shortened with half the pulse rise to $10\mu s$. But the magnetic pulse compression will only have an influence on the charging part of the pulse to the reactor. This is because the discharging current of the corona reactor doesn't go through the saturable inductor and thus the inductor has no influence on the discharging of the capacitance part of the compartment of the corona reactor. The compression is independent of the plate distance of the compartment of the corona reactor or the value of C_L, figure 4.34 shows what the difference is in the voltage waveforms. In this figure the voltage on compartment 1 and compartment 2 of the two compartment mpc corona reactor is shown. In figure 4.35 is the corona current shown with the total current and the current to each of the compartments of the two compartment mpc corona reactor.

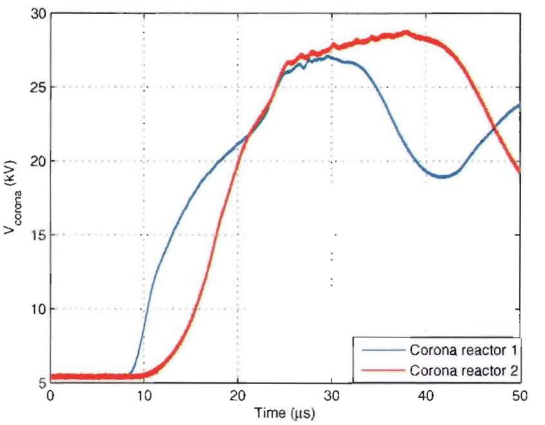

Figure 4.34: Time resolved voltages waveforms of the two compartment mpc corona reactor 9-9cm

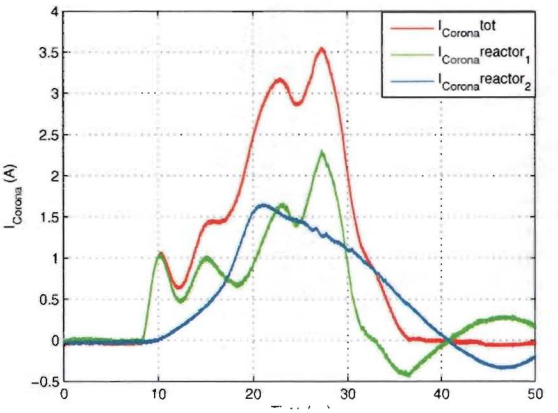

Figure 4.35: Time resolved current of the two compartment mpc corona reactor 9-9cm

The current of compartment 2 of the mpc corona reactor has an oscillation, see figure 4.36 for a multiple shot plot where the oscillation is clearly visible. This current causes also a small oscillation in the high-voltage on the two compartment mpc corona, which is shown in figure 4.37.

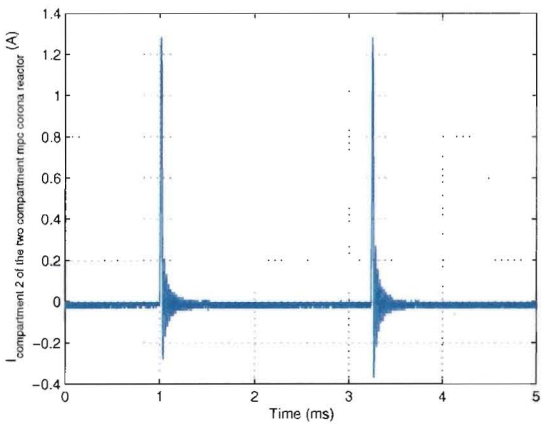

Figure 4.36: Time resolved corona reactor current of compartment 2 of the two compartment mpc corona reactor 10-10cm with multiple shots

The compression of the pulses can be adjusted by adjusting the point of saturation, but as told before the compression only works for the charging part of the corona reactor capacitance.

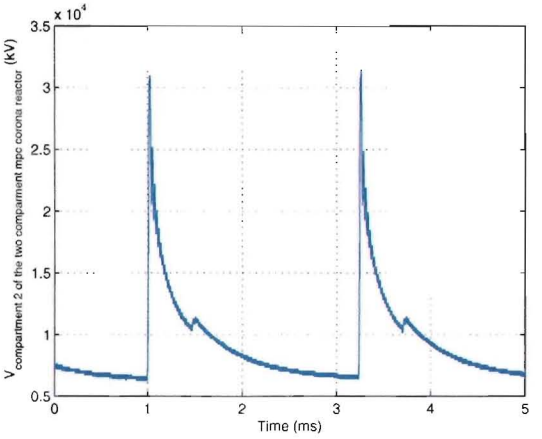

Figure 4.37: Time resolved corona reactor high-voltage of the two compartment mpc corona reactor 10-10cm with multiple shots

4.5.3 Ozone

It's logical that the amount of ozone concentration expressed in $[ppm]$ is about two times higher with the two compartment corona reactor and mpc corona reactor than with the one compartment corona reactors as made clear in figure 4.39. The two compartment corona reactor produces the same amount of ozone as the two compartment mpc corona reactor, but due to a difference in relative humidity between the two measurements the ozone production of the two compartment mpc corona reactor 10-10 cm is higher than the two compartment corona reactor (see figure 4.38[11]). The two compartment mpc corona reactors with different plate distance compartments produce the same ozone concentration as the one compartment corona reactors of the used different plate distance compartments are counted up together. This means that the ozone production isn't influenced by the fact that two compartments are connected together even when there are two different plate distances compartment used.

With the Ozone yield it's an other story, because the energy used in the two compartment mpc corona reactors isn't the same as twice the energy of the one compartment corona reactors even not if the energy values are counted up by each other when the two compartments of the two compartment mpc corona reactor have different plate distance compartments. This explains why the ozone yields of the two compartment mpc corona reactors are much better due to the fact that they use less energy compared to the one compartment corona reactors plus they also produce more ozone (see figure 4.39), this leads to the calculated (equation 4.2) values as shown in figure 4.40. But the most loudest plot is the ozone yield of the two compartment corona reactor 10-10 cm, even when the measured ozone concentration is about the same as with the two compartment mpc corona reactor. However the fact that the energy of the two compartment corona reactor (see figure 4.25) is much lower explains why the ozone yield of the two compartment corona reactor is so high.

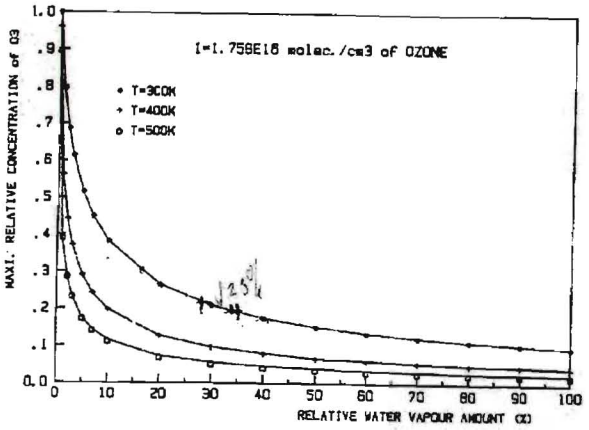

Figure 4.38: Maximum relative concentration of ozone versus relative water vapor amount ($100\% = 5.8e^{1}7 molecules/cm^{3}$) for various temperatures. [11]

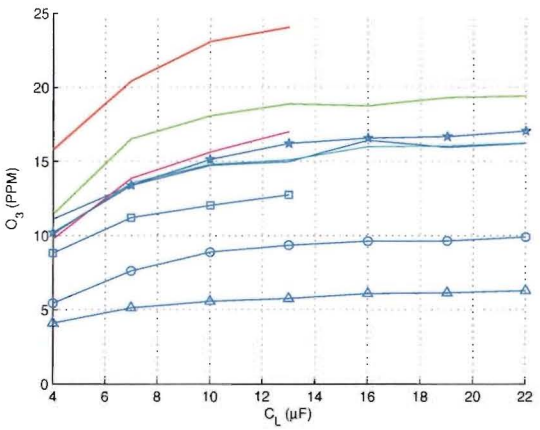

Figure 4.39: Ozone production of the two compartment mpc corona reactor with: Red: 9-9cm, Green: 10-10cm, Blue: 11-11cm, Cyan: 9-11cm and Magenta: 11-9cm, the two compartment corona reactor with: $\star$: 10-10cm and the one compartment corona reactor with: $\square$: 9cm, $\bigcirc$: 10cm, $\triangle$: 11cm

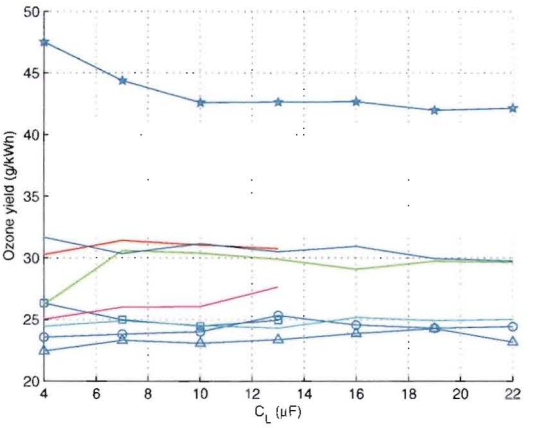

Figure 4.40: Ozone yield of the two compartment mpc corona reactor with: Red: 9-9cm, Green: 10-10cm, Blue: 11-11cm, Cyan: 9-11cm and Magenta: 11-9cm, the two compartment corona reactor with: $\star$: 10-10 cm and the one compartment corona reactor with: $\square$: 9cm, $\bigcirc$: 10cm, $\triangle$: 11cm

Chapter 5

Conclusions and Recommendations

5.0.4 Conclusions

After the experiments with the three setups, the one compartment corona reactor, the two compartment corona reactor and the two compartment mpc corona reactor the following conclusions can be made:

- The experiments with the different configurations, the one compartment corona reactor, the two compartment corona reactor and mpc corona reactor show that the two compartment corona reactor has the highest ozone production and the best ozone yield.
- The idea that with magnetic pulse compression, thus a pulsed high-voltage, the ozone production and the ozone yield would be better is refuted. Indeed the ozone production and ozone yield are with the two compartment mpc corona reactor better than with the one compartment corona reactor. But compare the two compartment corona reactor with the two compartment mpc corona reactor and it is shown that the two compartment corona reactor has much better results. The magnetic pulse compression did work as regards the compression of the high-voltage pulse, because there is indeed a shorter pulse rise time. But the fact that the magnetic pulse compression only works for the charging part of the corona reactor was a disappointment.
- The model for the matching of C_L with C_{Corona} didn't fulfill with the experiments due to a small transformer ratio and a V_{dc} on C_L.
- The $V_{dc_{Corona}}$ is determined by the size of the capacitance of the corona reactor. As C_{Corona} gets bigger $V_{dc_{Corona}}$ gets smaller. And also $V_{Corona}max$ is determined by the capacitance of the corona reactor but in the opposite direction, if C_{Corona} gets bigger $V_{Corona}max$ gets smaller.

5.0.5 Recommendations

For future work the next recommendations are made:

- Experiments with a transformer with a higher transformer ratio. The used transformer for the shown results was 36 with a maximum of 36 kV which is quit low.
- A profound study of the patent pending magnetic pulse compression, due to the fact that a better magnetic pulse compression can be achieved.

Acknowledgement

The presented work couldn't be done all by myself, that's why I would like to thank some people. First of all Dr. Ing. Guus Pemen and Prof. Dr. Ir. Jan Blom for giving me to opportunity to do my Masters project in there research chair: Electrical Power systems. Dr. Keping Yan for his advice and discussions about the circuit and his proposals for solutions. Also Ir. Hans Winands for the advice, transfer of knowledge and the use full discussions about the project and other cases. Zhen Lui I would like to thank for time-sharing his oscilloscoop and other measurement equipment, also his advice and knowledge about specific cases were a warm welcome to me.

Not everything of the project could be modeled, so the experiments did bring some surprises some times, like breakthroughs. Also mechanical and construction problems were things which needed to be dealt. This made the project every time a challenge and kept me sharp. Due to the problems on other arias I got also help from the supporting staff of the research group which I would like to thank them for. And finally my fellow students of our own faculty as well the students of the chemistry department for there input on the problems I suffered.

Bibliography

[1] K. Yan. Inrichting voor het genereren van corona-ontladingen. NL 1024408, 30th September 2003. Patend pending.

[2] G.J.J. Winands, Z. Liu, A.J.M. Pemen, E.J.M. van Heesch, and K. Yan. Long life-time triggered sparkgap switch for repetitive pulsed power applications. In *Rev.Sci.Instrum.*, volume 76, page 085107, August 2005.

[3] K. Yan, G.J.J. Winands, Z. Liu, E.J.M. van Heesch, and A.J.M. Pemen. Comparison of two-type corona plasma energization techniques: ultrashort and dc/ac power sources. In *Conference Record of the 2005 IEEE Industry Applications Conference Fortieth IAS Annual Meeting IEEE Cat. No. 05CH37695*, volume 3, pages 1840–1844, 2005.

[4] G.J.J. Winands, K. Yan, S.A. Nair, A.J.M. Pemen, and E.J.M. van Heesch. Evaluation of corona plasma techniques for industrial applications: Hpps and dc/ac systems. In *Plasma-Processes-and-Polymers*, volume 2, pages 232–237, 31 March 2005.

[5] Keping Yan. *Corona plasma generation.* PhD thesis, Technische Universiteit Eindhoven, Department Electrical Engineering, Capacities group Electronic Power Systems, 2001.

[6] K. Yan, E.J.M. van Heesch, A.J.M. Pemen, P.A.H.J. Huijbrechts, F.M. van Gompel, H. van Leuken, and Z. Matyas. A high-voltage pulse generator for corona plasma generation. In *IEEE Transactions on Industry Applications*, volume 38, pages 866 – 872, May-June 2002.

[7] Sreejit A. Nair. *Corona plasma for tar removal.* PhD thesis, Technische Universiteit Eindhoven, Department Electrical Engineering, Capacities group Electronic Power Systems, 2004.

[8] S.A. Nair, K. Yan, A. Safitri, A.J.M. Pemen, E.J.M. van Heesch, K.J. Ptasinski, and A.A.H. Drinkenburg. Streamer corona plasma for fuel gas cleaning: comparison of energization techniques. In *Journal-of-Electrostatics.*, volume 63, pages 1105–1114, Oct. 2005.

[9] Keping Yan, Daisuke Higashi, Seiji Kanazawa, Toshikazu Ohkubo, Yukiharu Nomoto, and Jen-Shin Chang. No_x removal from air streams by a superimposed ac/dc energized flow stabilzed streamer corona. In *Trans. IEE of Japan*, volume 118-A, pages 948–953, September 1998.

[10] S. A. Nair, A. J. M. Pemen, K. Yan, F. M. van Gompel, H. E. M. van Leuken, E. J. M. van Heesch, K. J. Ptasinski, and A. A. H. Drinkenburg. Tar removal from biomass-derived fuel gas by pulsed corona discharges. In *Fuel Processing Technology*, volume 84, pages 161–173, 15 November 2003.

[11] R. Peyrous. The effect of relative humidity on ozone production by corona discharge in oxygen or air - a numerical simulation - part II: Air. In *Ozon Science & Engineering*, volume 12, pages 41–64, 1990.

Appendix A

Table of component values

Table A.1: Model components values

C_0	$3.3mF$ ($2 \cdot 6.6mF$ serie)
L_1	$21\mu H$
C_L	$4 - 7 - 10 - 13 - 16 - 19 - 22\mu F$
L_2	$18\mu H$
N (Transformer)	36
C_{Corona}	$250pF$

Table A.2: Components values

C_0	$3.3mF$ ($2 \cdot 6.6mF$ serie)
L_1	$21\mu H$
C_L	$4 - 7 - 10 - 13 - 16 - 19 - 22\mu F$
L_2	$18\mu H$
$L_{prim}HSP - trafo$	$2.31mH$
L_{sec}	$3H$
N (Transformer)	36
Th_1, Th_2, Th_3	thyristor ABB type 5 STF o8F2060
L_4	1.7 mH
R_4	$6.8k\Omega$
R_1	50Ω
C_1	$50nF$
R_2	50Ω
C_2	$50nF$
R_3	50Ω
C_3	$50nF$
C_{Corona}	$9cm : 240 \sim 250pF$ $10cm : 230 \sim 243pF$ $11cm : 225 \sim 234pF$ $10 - 10cm : 539 \sim 534pF$

Appendix B

Matlab formulas

The formulas are shown as used in Matlab 7.0.

Primary Voltage & Current
$V_{primary} = (C400000 - C300000). * 1000$
(Voltage probe gives $1V = 1kV$ with $R_{scoop} = 1M\Omega$)
$I_{primary} = (C200000). * 20$
(Rogowski coil gives $1V = 0.5A$ with $R_{scoop} = 50\Omega$)

Secondary Voltage & Current
$V_{secondary} = (C400000). * 1000$
(Voltage probe gives $1V = 1kV$ with $R_{scoop} = 1M\Omega$)
$I_{secondary} = (C200000). * 20$
(Rogowski coil gives $1V = 0.5A$ with $R_{scoop} = 50\Omega$)

Power
$P_{primary} = V_{primary} \cdot I_{primary} = (C400000 - C300000). * C200000. * 1000. * 20$
$P_{secondary} = V_{secondary} \cdot I_{secondary} = C400000. * C200000. * 1000. * 20$

Energy
$E_{primary} = \int P_{primary} = cumsum((C400000 - C300000). * C200000. * 1000. * 20. * d)$
$E_{secondary} = \int P_{secondary} = cumsum(C400000. * C200000. * 1000. * 20. * d)$
With B = cumsum(A) returns the cumulative sum along different dimensions of an array. If A is a vector, cumsum(A) returns a vector containing the cumulative sum of the elements of A. d is the time of each step of the power vector.

Efficiency
$\eta = \frac{E_{primary}}{E_{secondary}}$

Ozone production

$PPM = Measurements \times \rho \times 1000$
$Measurements = [mol/m^3]$
$\rho = \frac{m}{V} = 0,002144 \frac{g}{cm^3}$

Ozone yield

$Ozoneyield = \frac{Measurements \times M \times V \times 1000}{P_{plasma}}$
$Measurements = [mol/m^3]$
$M = molecular\ mass[g/mol]$
$V = flow[m^3/h]$
$P_{plasma} = energy\ per\ pulse\ [J] \times rep\ rate\ [s^{-1}]$
$Ozoneyield = [g/kWh]$